METHODS FOR IMPROVED KINEMATIC MEASUREMENTS OF THE LOWER EXTREMITIES

A Thesis

presented to

the Faculty of the Graduate School

at the University of Missouri-Columbia

In Partial Fulfillment

of the Requirements for the Degree

Master of Science

---

by

ROSE SCHAUFFLER

Dr. Trent Guess, Thesis Supervisor

MAY 2022

The undersigned, appointed by the dean of the Graduate School, have examined the thesis entitled

Methods for Improved Kinematic Measurements of the Lower Extremities

presented by Rose Schauffler,

a candidate for the degree of Master of Science,

and hereby certify that, in their opinion, it is worthy of acceptance.

Dr. Trent Guess

Department of Physical Therapy and Department of Orthopedic Surgery

Dr. Jamie Hall

Department of Physical Therapy

Dr. Heather Hunt

Department of Biological Engineering

DEDICATION

I am dedicating this thesis to my family and close friends. A special thank you to my loving mother who has always supported me no matter what path I choose. My aunts and uncles – Ed, Darla, Les, Linda, Doris, and Fred – also consistently offered their support and words of wisdom. I would also like to dedicate this work to the memory of my grandmother who encouraged curiosity and a love of learning early on and to my Aunt Marion who left behind a love of music and the fine arts.

ACKNOWLEDGEMENTS

First, I would like to thank Dr. Guess for his guidance not only during my graduate education but also for his mentorship during my undergraduate years and for guiding me to the field of biomechanics. Dr. Jamie Hall has also provided great insights throughout this process. Kylee Rucinski was extremely helpful with finding patients at the MOI and facilitating data collection times. My entire thesis committee has also given many great suggestions – Dr. Guess, Dr. Hall, and Dr. Heather Hunt. Finally, the faculty and staff of the Physical Therapy Department and Motion Analysis Center have been conducive to a wonderful working environment in which to do research.

List of Tables

List of Figures

List of Abbreviations

ACL	Anterior Cruciate Ligament
ACLd	Anterior Cruciate Ligament deficient
IRB	Institutional Review Board
LSD	Lateral Step Down
MKATS	Mizzou Knee Arthrometer Testing System
PFP	Patellofemoral Pain
SLS	Single Leg Squat
SUO	Step Up and Over

TABLE OF CONTENTS

Abstract

An understanding of knee dynamics is vital to treat neurological and musculoskeletal conditions that affect the lower extremities and achieve peak performance from athletes. To obtain and analyze kinematics and kinetics of the knee, clinicians and athletic trainers require accurate, accessible measurement devices. To assess the functionality of one such device, the Mizzou Knee Arthrometer Testing System (MKATS), dynamic motion studies were carried out on healthy, ACL deficient, and patellofemoral pain populations. To assess the validity of the MKATS, the device output was compared to data collected using a SimVitro robotic manipulator. Through this process, discussions with clinicians, technicians, and participants resulted in modifications to both the software and hardware of the device to improve fit and usability. The following thesis summarizes the findings of the dynamic and cadaver motion studies, and the modifications to the device.

We found decreased flexion and internal rotation at specific points ($p<0.05$) of the cycle for all dynamic activities for both clinical groups compared to the healthy control group. Due to unperceived amounts of skin artifact and joint laxity, the results of the cadaver study were inconclusive. The MKATS was able to accurately detect kinematic differences in the live study groups and has promise as a useful tool for orthopedic surgeons, physical therapists, and athletic trainers to screen for abnormal dynamics and track treatment success. Further studies utilizing computed tomography on live participants will be needed to further validate the MKATS. The development of such devices is crucial to improve the quality of advice from healthcare and athletic performance specialists.

1. Introduction

1.1 Motivation

There is a strong link between athletic performance and biomechanics. Biomechanics gives us great insight into the development of power in a golf swing[14,51], the intricate combination of muscle activations in a violinist's shift[64], and the loading conditions during an anterior cruciate ligament (ACL) rupture in a soccer player[44,45]. Looking at a combination of kinetics and kinematics provides a scientific basis and justification for the development of training, teaching, and treatment methods for athletes, musicians, and those undergoing rehabilitation therapies[37]. The reasoning behind holding your instrument or golf club a certain way goes beyond historical practices and can be justified by minimal loading at a specific joint or lower activation in a particular muscle group[9]. Understanding the connection between human motion and performance is vital to developing techniques and equipment to minimize injuries and maximize execution[37].

Injuries are extremely common in string players[48] and athletes[14,50,57]. The study of knee dynamics is particularly relevant for sports and activities that involve cutting maneuvers and power development such as soccer or basketball as individuals are at increased risks of injury[32,50]. Understanding how healthy knees move can help coaches train to maintain good kinematics and clinicians work to bring injured knees back to that state[50]. However, effective collection of such data may be limited by the scope of current devices. A known connection between motion and performance provides a solid basis of theory for increasing performance but is only applicable in generalized terms. The development of technology to increase accessibility to dynamic kinematic data promises to improve individualized training and treatment.

1.2 Background

There is a high prevalence of musculoskeletal disorders affecting the knee such as patellofemoral pain[57] and ACL injury[30,49]. These disorders are often characterized by differences in stability and altered knee biomechanics[1,5,45,46]. For patients with ACL injuries, decreased stability is evident in altered internal-external rotation angles[4]. The defining features for patients with PFP are altered biomechanics, a compensation developed over time in order to avoid pain elicited during activities that activate the quadriceps[2,66]. Collection and analysis of knee rotation angles about the 3 primary axes (flexion/extension, internal/external rotation, and abduction/adduction rotation) can provide clinicians insight into underlying conditions of the knee[45,58]. In order to analyze and compare data collected from various methods, it is important to use a standard coordinate system to describe knee motion[21,27].

The coordinate system described by Grood and Suntay in 1983 continues to be one of the most popular coordinate systems in use to describe knee motion[27,33]. This system is comprised of two fixed body axes and one "floating" axis. The first axis is fixed to the femur and describes flexion and extension while the second is fixed to the tibia and describes internal and external rotation. The third non-fixed axis is perpendicular to the other two axes and describes varus and valgus rotation (also known as abduction/adduction rotation)[21,27]. These axes are summarized in Figure 1.

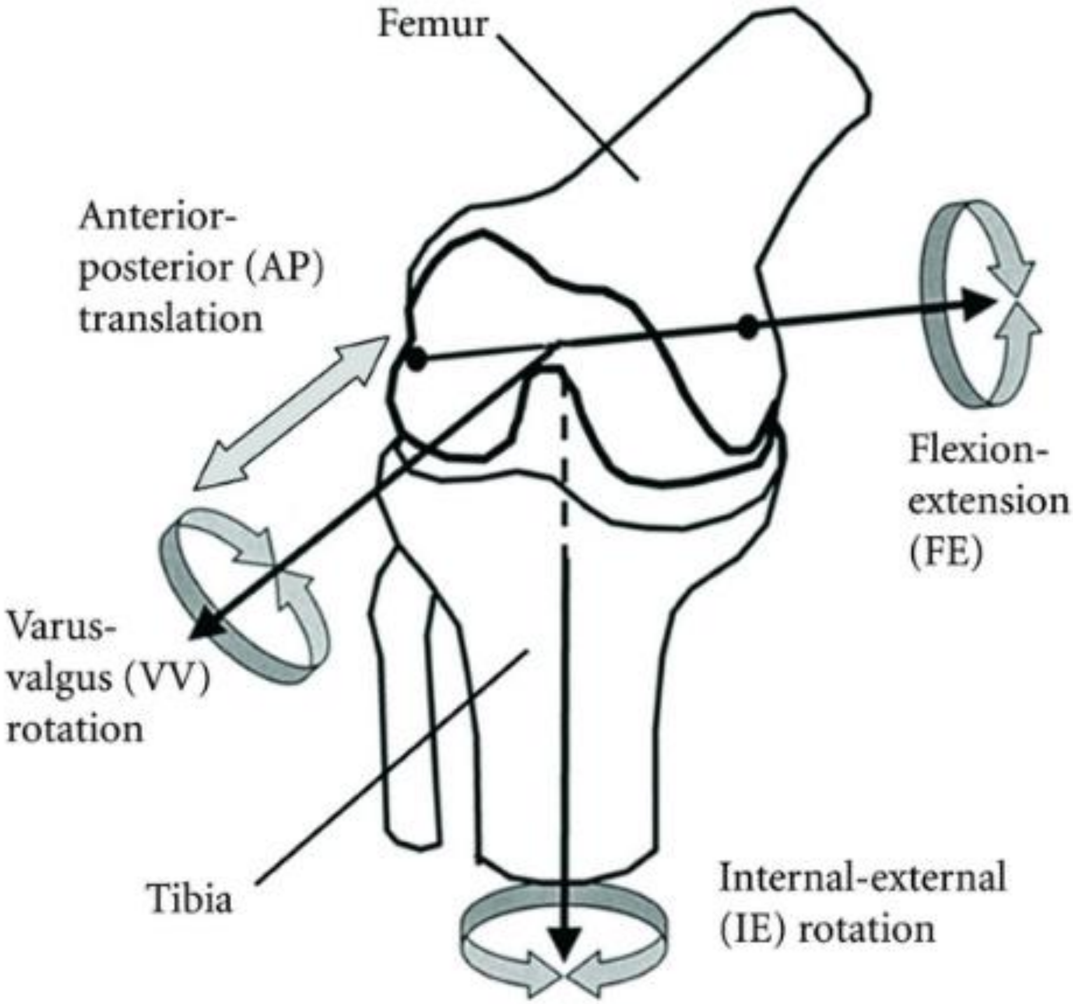

Figure 1. Directions of the rotations and translations according to Grood and Suntay's coordinate system definition of the knee[21]. The flexion-extension axis is fixed to the femur and the internal-external axis is fixed to the tibia. The varus-valgus (or abduction-adduction axis) is perpendicular to the other axes.

Existing methods to measure knee rotation include forms of 3D motion software such as Vicon Nexus. Physical retroreflective markers are placed on the skin on specific landmarks[1]. Sets of markers are used to define anatomic rigid bony bodies for dynamic analysis. For knee biomechanics, a functional model including Symmetrical Axis of Rotation Analysis (SARA) and Symmetrical Center of Rotation Estimation (SCoRE) methods is often used to define the axes described above[27,33]. For both methods, the optimal common shape technique is applied to each segment (i.e. femur, tibia, and pelvis) to obtain rigid bodies based on the skin markers[33]. The SCoRE method then uses an optimization algorithm to estimate the hip joint center while the SARA method uses a different optimization algorithm to estimate the knee joint center[33]. When paired with force plates, these data collection methods have proven to be extremely robust and provide a large body of information including forces, moments, power, and joint angles[18,33]. While these systems are effective, they can cost upwards of $200,000 and cannot be transported requiring patients to enter a laboratory setting to be evaluated. Due to skin artifact, the accuracy of non-sagittal knee motion is also prone to error[7]. Special training on the software to collect, process, and interpret data is another roadblock to ease of use by clinicians and often such extensive data is not necessary for clinical diagnoses.

One method to reduce skin artifact is the use of bone pins[6]. Often these are used in conjunction with a motion capture software and similar methods to the SCoRE and SARA methods. However, the invasive nature of the pins exposes patients to additional risks and discomfort[6].

Dual fluoroscopy is another expensive, but robust method to analyze knee motion[39,61,62]. The method consists of taking x-rays in real time in 2 different planes as the participant goes through functional tasks[62]. 3D models of the knee obtained from MRI or CT scans can then be fit to the biplanar x-ray images and used to calculate the kinematics of the knee[39,61,62]. As the images are directly of the bones, there is little motion artifact such as that which may be present in 3D motion analysis with surface retroreflective markers[39]. However, this method is limited by portability and the expertise needed to process such data[62]. Additionally, although low dosage, radiation exposure can be a risk for patients and operating staff[60].

There are various knee arthrometers such as the KT-2000 and the Genourob[35]. However, these devices are not suitable for dynamic measurements due to their rigid, bulky nature and limit which tests can be used[34,56]. Many of these devices only measure static anterior displacement and were found to have a level of subjectivity depending on the user[56]. While significantly less expensive than dual fluoroscopy or other motion capture methods, these arthrometers are not effective in dynamic settings such as athletic activities and other daily functional tasks[34]. In addition, many of these products have been discontinued by their manufacturers and as such are difficult to obtain[34].

Method	Description	Limits	Advantages	Citations
Marker based motion capture	Retroreflective markers are placed, data is collected, processed, and interpreted using various algorithms.	- Expensive ($200,000+) - Extensive training required - Skin artifact - Not portable	- Triplanar motion - Analysis of multiple joints - Can include kinetic analysis	1,7,18,27,33
Dual fluoroscopy	Biplanar x-ray images are fit to 3D geometries obtained with MRI or CT scans	- Expensive - Exposure to radiation - Time consuming - Tasks limited by capture space - Not portable	- High accuracy with minimal motion artifact - Triplanar motion	39,61,62
Arthrometers	Patients are guided to a position, the arthrometer is strapped in place, and a force is applied	- Typically static measurements - Single plane motion - Discontinued products	- Price - Portability	34,35,56
MKATS	Device is fitted to the patients knee and calibrated before collecting	- Only knee kinematics are measured (no other joints) - Software development	- Price - Portability - Triplanar motion	23,24

	dynamic motion data			

Table 1. Summary of current methods to measure knee motion with limits and advantages. While the MKATS is limited to measurements of tibiofemoral motion, it is cheaper and more portable which is important in a clinical setting.

The MKATS is a novel design of a knee arthrometer. It consists of a femur clamp and a tibia clamp which can be easily placed by a clinician during a data collection session. Each clamp has an electromagnetic sensor that detects the clamps' positions relative to each other. A visualization of the two sensors can be seen in Figure 2. These sensors use the Polhemus Patriot motion tracking system to collect raw data on the relative positions. Custom algorithms are then applied to the raw data to calculate joint angles in the three primary knee axes as described above. This gives a cheaper, more portable alternative to other knee kinematic measurement methods by providing real time data. Unlike methods such as dual fluoroscopy and instrumented marker-based motion analysis, the MKATS does not require other anatomical features (i.e. femoral head anatomy) to calculate rotation angles.

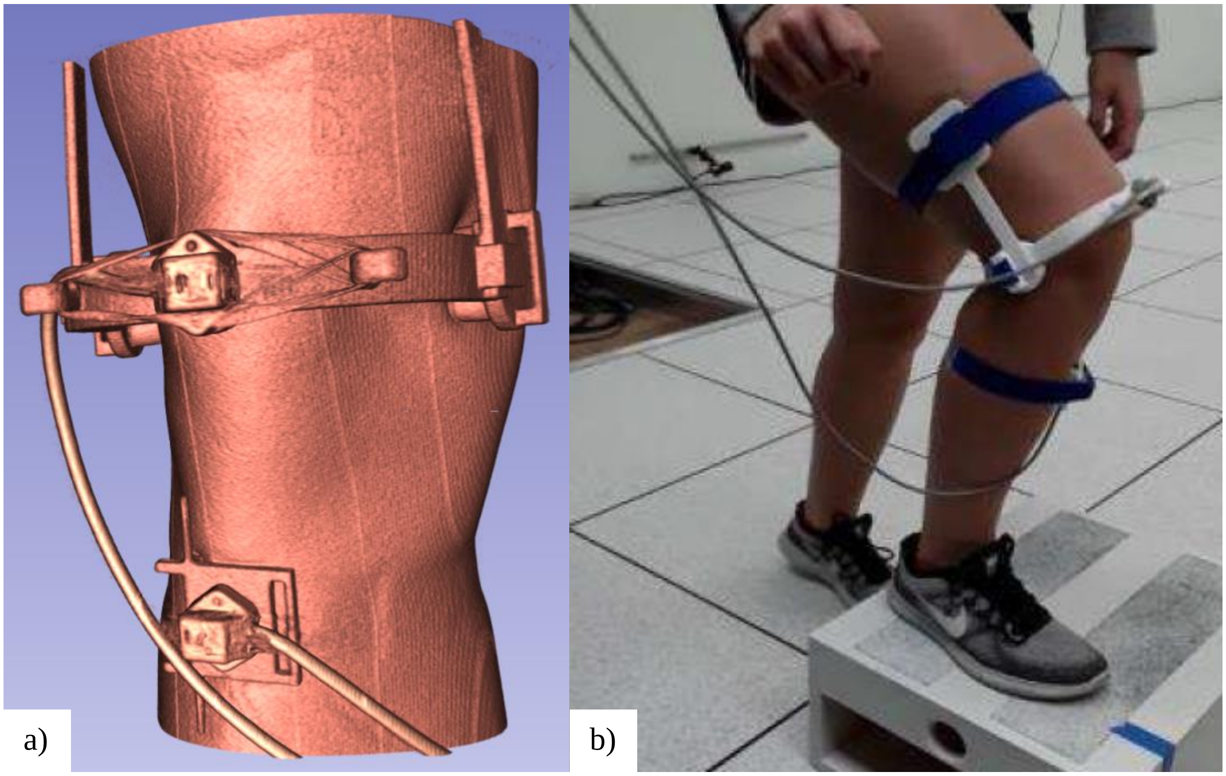
a) b)

Figure 2. (a) Model of the Mizzou Knee Arthrometer Testing System (MKATS). The upper clamp is positioned across the femoral condyles while the lower clamp is positioned along the anterior tibial crest beneath the tibial tuberosity. (b) Prototyped device on a research participant. The main clamps are 3D printed with the associated electromagnetic sensors attached. Both clamps are secured with straps.

The MKATS was designed for use by clinicians such as physical therapists, orthopedic surgeons, and athletic trainers who evaluate and treat conditions of the knee. Joint angles collected during weight bearing functional activities may have the following clinical applications: diagnosis of ligament injuries, diagnosis of iliotibial band syndrome, diagnosis of osteoarthritis, screening for ACL injury risk, screening for return to sports, screening for patellofemoral pain, and screening for osteoarthritis. A small market analysis has been performed to identify appropriate testing procedures, but there will likely be a more thorough one required prior to putting the product on the market in order to comply with the Food and Drug Administration (FDA) and other regulatory agencies.

Functional tasks frequently used in the evaluation of common knee conditions such as PFP and ACL injuries were compared to identify an appropriate testing procedure for objective 1. Such tasks look to identify knee instability and determine if individuals are prepared to return to sports[20,66]. In looking at how the knee is loaded during functional tasks for the diagnosis and screening of these ailments, a comprehensive list can be made. This list includes standard tests such as single leg squats[2], dual limb squats[2], y balance tests[4], single leg hop tests[20,29,54], triple hop tests[54], crossover hop tests[20,38], step up tasks[2,52,53], lateral step downs[2,52,53], and drop cut jumps[20]. Currently evaluation with these tasks primarily relies on limited information such as the patient's subjectively reported pain or the clinician's visual assessment during the activity[32,66]. As such, objective kinematics could be greatly beneficial to clinicians evaluating knee function. Due to the relationship between internal knee loads and joint stability, the use of dynamic tasks with internal loading are effective methods for diagnosis[28,35].

1.3 Objectives and Aims

We hypothesized that the Mizzou Knee Arthrometer Testing System (MKATS) will prove to be an effective, noninvasive method to measure joint angles during functional activities. The primary objective of this study was to validate and assess the functionality of the MKATS so that it may be used by clinicians. This was achieved through a series of functional tests and comparisons to existing data sets and methods. The two primary objectives were to show that the MKATS is functional and to validate it with other existing methods. Additional objectives were to increase the modularity of the data collection software and assess the marketability of the device.

Objective I: *Assess functionality*

Demonstrate that the MKATS can adequately collect reasonable knee rotation data for the three primary axes for a series of functional tasks in a clinical setting. These three axes describe flexion/extension, internal/external rotation, and abduction/adduction rotation. To assess functionality of the MKATS, the following aims were met:

(1) Development of an appropriate testing protocol that covers a range of functional motion about the knee.

(2) Collection and analysis of control participant data to act as a baseline.

(3) Collection and analysis of clinical patient data from populations with patellofemoral pain and ACL deficiencies.

Objective II: *Validation*

Show that data collected from the MKATS is reliable and clinically relevant to assess musculoskeletal disorders and abnormal motion of the knee joint. This included comparing data to that collected from other existing standard methods with known validation. For this objective, the following aims were met:

(1) Simultaneous data collection on cadaver specimens with both SimVitro and MKATS systems.

(2) Simultaneous data collection with CT scans and the MKATS.

Objective III: *Modularity*

The primary program used to collect data for the MKATS uses a custom C# code that interfaces with the Unity Game Engine. It is limited by being unidirectional with fixed data collection times. Additionally, the program holds each sample for two data collection points thus decreasing the frequency of recorded values. To increase modularity of the user interface and fidelity of the data stream, the following was done:

(1) Development of a new code to collect data with adjustable collection times. Users will be able to input file names and data collection time.

Objective IV: *Explore marketability*

Interact with clinicians and potential future users of the MKATS to explore customer segments and determine a value proposition model.

(1) This was done in part with the regional NSF Innovation Corps program through interviewing potential customer segments including physical therapists and athletic trainers specializing in orthopedic practice.
(2) A multidisciplinary team participated in training sessions and summarized the findings in a value proposition format to be presented and critiqued by other groups.

3. Methods

3.1 Live Participant Trials

3.1.1 Participants

University Institutional Review Board approved this study design. Three groups of participants were recruited – healthy control, ACL deficient (ACLd), and those with PFP. Inclusion criteria for the control group included above 18 years of age with no history of ACL injury or patellofemoral pain. Inclusion criteria for the ACL group included above 18 years of age with a known ACL deficiency. Inclusion for the PFP group similarly included known diagnosis of PFP. Exclusion criteria included incarceration, incapable of making medical decisions, and pregnancy. Participants were asked about exclusion criteria prior to taking part in the study and provided written consent.

3.1.2 Device

Electromagnetic motion sensors were used to collect tibiofemoral motion data (Polhemus Patriot System; Polhemus, Colchester, VT). Sensors were secured to custom nylon fixtures on the bony surfaces of the distal femur and proximal tibia. The femoral fixture was compression clamped to the medial and lateral epicondyles and further secured with elastic strapping. The tibial unit was fixated to the anterior tibial crest immediately inferior to the tuberosity and secured with elastic strapping (see Figure 2. (a) Model of the Mizzou Knee Arthrometer Testing System (MKATS). The upper clamp is positioned across the femoral condyles while the lower clamp is positioned along the anterior tibial crest beneath the tibial tuberosity. (b) Prototyped device on a research participant. The main clamps are 3D printed with the associated electromagnetic sensors attached. Both clamps are secured with straps.). By targeting these bony landmarks, skin and motion artifact concerns were minimized. A custom Unity code was used to interface with the Patriot and convert the raw orthogonal data into anatomically relevant joint angles consistent with the Grood and Suntay model[21]. Two coordinate axes are from the local coordinate systems of the tibial and femoral segments while the third axis is a cross product of those axes. The femoral epicondyles define the axis of flexion, and the long axis of the tibia defines the axis of internal rotation. The cross product of these axes defines abduction-adduction rotation.

3.1.3 Data Collection

All participant groups were asked to perform dynamic tasks after being fitted with the clamps during a single data collection. The clamps were placed by those trained to palpate the previously described bony landmarks. ACL deficient and PFP participants only performed tasks on the affected limb while control participants performed tasks bilaterally. Prior to testing, ACL deficiency or diagnosis of PFP and ability to perform tasks was confirmed by an orthopedic surgeon for the clinical groups. Participants first performed range of motion and static tasks followed by a minimum of three trials each of step up and over, posteromedial Y-balance, posterolateral Y-balance, lateral step-down, medial single leg squat, and lateral single leg squat tasks. Table 1 summarizes the tasks with a brief description of each.

Task Name	Description	Specific Equipment/Setup
Step up and over	The participant steps up and over a box in a continuous motion, pausing between each cycle.	20 cm height wooden box.
Y balance posterolateral	The participant balances on one leg while sliding the other leg behind and across the body along fixed line as marked on the floor.	Three lines on the floor situated at 135˚, 135˚, and 90˚.
Y balance posteromedial	The participant balances on one leg while sliding the other leg behind and to the side along a fixed line as marked on the floor.	Three lines on the floor situated at 135˚, 135˚, and 90˚.
Single leg squat turned medially	The participant turns upper body 90˚ toward the leg they are squatting on.	The participant will begin on a floor marking and be asked to rotate 90˚ toward the wall nearest to the squatting leg.
Single let squat turned laterally	The participant turns upper body 90˚ away from the leg they are squatting on.	The participant will begin on a floor marking and be asked to rotate 90˚ toward the wall farthest from the squatting leg.

Lateral step down	The participant will stand atop a box on a single limb with the other limb positioned over the floor. They will then bend the knee of the first limb to gently touch the heel of the other limb to the floor before rising again to the starting position.	20 cm height wooden box.

Table 2. Summary of dynamic trials and descriptions performed by voluntary participants.

3.1.4 Data Analysis

Custom Matlab code (MATLAB R2019b; MathWorks, Inc, Natick, MA) was used to identify cycle start and end points and extract trial cycles (see Figure 3. Flexion-extension angle over time for representative participant during step-up and over task. Three cycles were identified for each trial. Stars represent chosen cycle peaks. Circles represent the start of the cycle and plus signs represent the end of the cycle.). Step up and over cycles were normalized to 151 data points while all other tasks were normalized to 101 data points by fitting to a cubic spline. Ensemble averages of three clean trials for each task were calculated for all participants. Discrete TF motion values and cycle times were compared between left and right control, and bilateral control and clinical group data sets using paired t-tests for each normalized data point. The Wilk-Shapiro test assured normal distribution of the data. Discrete TF values were compared at every normalized data point. Statistical significance was identified as $p<0.05$ *a priori*. Values were seen as statistically significant with $p < 0.05$. All calculations were performed in Matlab.

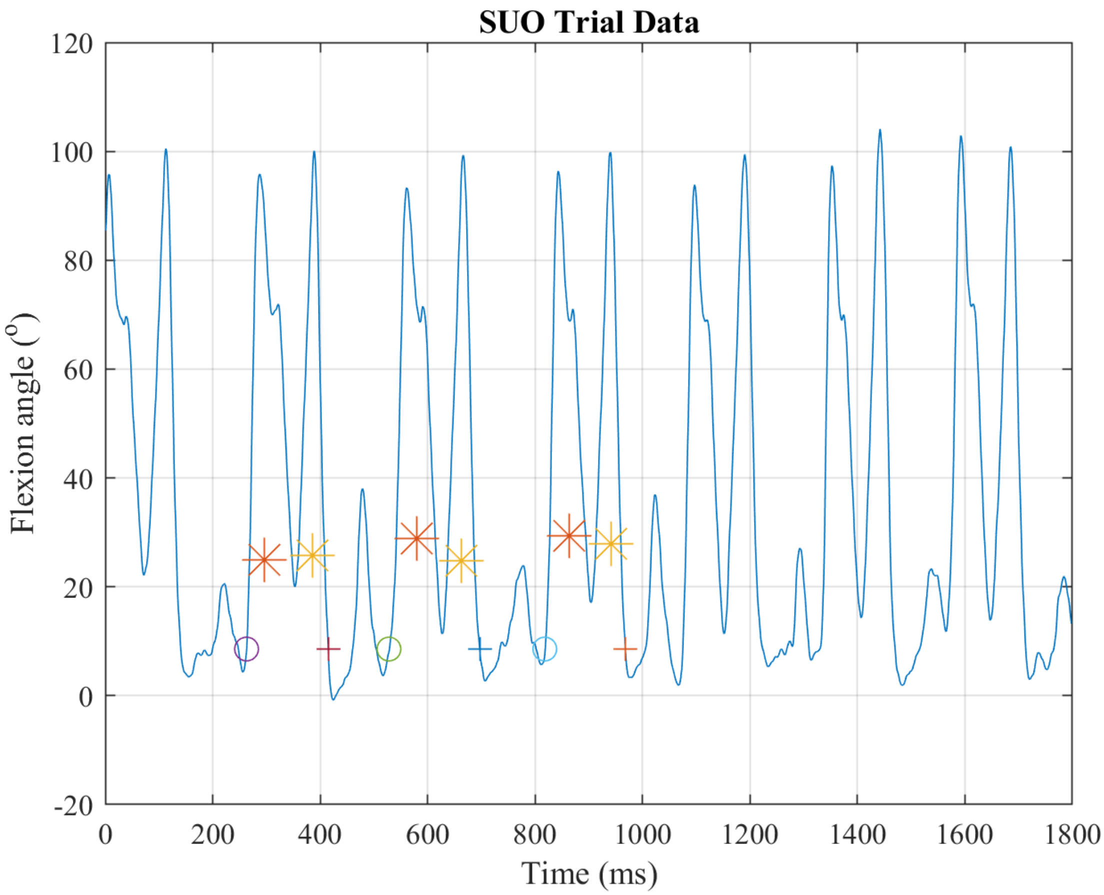

Figure 3. Flexion-extension angle over time for representative participant during step-up and over task. Three cycles were identified for each trial. Stars represent chosen cycle peaks. Circles represent the start of the cycle and plus signs represent the end of the cycle.

3.2 Cadaver Trials

3.2.1 Specimens

Specimens were obtained with IRB approval. All fresh-frozen specimens were male (60.3 ± 8.65 years, 141 ± 36.4 lbs.) and went from mid-femur to mid-tibia. Flesh was removed from the femur and tibia 15cm down to prepare the specimens for potting in woods metal. The remaining fibula was removed from the inferior tibia. All ligaments, muscle, tendons, and skin remained over the knee joint.

3.2.2 Devices

A simVITRO robotic testing system (Cleveland Clinic, Cleveland, OH) with a KUKA KR300 r2500 Ultra robot (Kuka, Ausburg, Germany) and an Omega 160 IP65 load cell with a SI-1000-120 calibration (ATI Industrial Automation, Apex, North Carolina, US) was used to apply the controlled loads and motions. The potted specimens were loaded into the testing system and the system was calibrated. Each specimen underwent simulation of internal-external rotation, varus-valgus rotation, and flexion-extension rotation. Specimens were also subjected to a simulated pivot shift. This is a common test utilized by clinicians to diagnose rotatory instability related to ACL tears because it simulates the event that occurs during ACL rupture[63]. The knee is flexed from 0˚ to 90˚ of flexion while applying external rotation stress to the tibia and an abduction stress to the knee[3].

See section 3.1.2 for a description of the electromagnetic sensors and clamps used collectively as the Mizzou Knee Arthrometer Testing System (MKATS). The MKATS was fitted to the specimen prior to data collection start and cycles of each task were collected simultaneously using the SimVitro and MKATS systems. A custom code was used to record the Patriot system data stream.

3.2.3 Data Collection

All specimens were loaded into the robotic manipulator and fitted with the MKATS clamps during a single data collection. The clamps were placed by those trained to palpate the previously described bony landmarks. Data were collected simultaneously from the load cells and MKATS system to be later compared.

3.2.4 Data Analysis

No in-depth analysis was performed as cadaver data was not comparable to live participants. Cursory comparison of load cell data from SimVitro and MKATS output was not comparable which led to pursuit of another validation method. MKATS data was collected simultaneously with CT scans for later joint angle comparison.

3.3 Software solution

An alternate program was written in C++ using the Polhemus Developer Interface (PDI). It was modified from the sample program that used Microsoft Foundation Classes (MFCs) to record data in metric units and to record quaternions instead of Euler angles. This program was used in the cadaver trials to collect joint angle data and is more modular than the Unity code. The data stream from the Patriot can be collected for a set amount of time in minutes or seconds and is recorded in a .txt file.

4. Results

4.1 Dynamic Motion Tests In Vivo

The step-up and over and lateral step-down tasks produced the cleanest data. As such, those data sets were analyzed in greater detail. Some participant data sets had to be excluded on a trial by trial basis due to sliding of the femoral clamp or participant inability to perform certain tasks. Compensation mechanisms for balance on the twisted squats varied greatly among participants. Due to the timing of the Y-balance tasks, most participants only had two posteromedial and two posterolateral trials. For all other tasks, three trials for each task were used in ensemble averages.

4.1.1 Participant Demographics

Twenty control participants (n=20, 14 female, 25.6 ± 4.96 years), twenty ACL deficient patients (n=20, 8 female, 31.3 ± 10.5 years), and twenty PFP patients (n=20, 10 female, 32.6 ± 10.3 years) were recruited for this study. Within the ACLd group there were 10 right and 10 left ACL deficient knees. The ACLd group had 2 outliers with regards to injury timing. Outliers were identified as any data points 1.5 times below the first quartile or above the third quartile. Demographic statistics were recalculated excluding these outliers. Within the PFP group, there were 14 right and 6 left affected knees.

	Control	**ACLd**	**ACLd without outliers**	**PFP**
Gender	14 female, 6 male	8 female, 12 male	8 female, 10 male	10 female, 10 male
Age	25.6± 4.96 years	31.3 ± 10.5 years	30.3 ± 10.4 years	32.6 ± 10.3 years
Weight	150 ± 27.5 lbs	192 ± 30.7 lbs	191 ± 32.3 lbs	178.1 ± 43.6 lbs
Height	66.8 ± 3.30 inches	68.4 ± 3.77 inches	68.9 ± 3.55 inches	68.2 ± 3.9 inches
PROMIS Physical Function	NA	40.5 ± 6.11	40.9 ± 6.32	NA
Affected Knee	NA	10 right, 10 left	9 right, 9 left	14 right, 6 left
Prehab	NA	2 some prehab, 18 none	2 some prehab, 16 none	NA
Injury to Data Collection	NA	17.7 ± 34.5 months*	6.29 ± 5.33 months	8.55 ± 5.16 months
Contralateral Knee History	NA	3 with history	2 with history	3 with history
Repeat Injury	NA	9 repeat, 11 primary	8 repeat, 11 primary	NA

Table 3. Summary of demographic data for participants. (*) Strongly affected by 2 outliers injured over a decade prior to data collection.

4.1.2 Step Up and Over

Table 4 summarizes the p-values during the step up and over task for all participant groups.

	LR			ACLd			PFP		
% of Cycle	Flex/Ext	Int/Ext	Ad/Ab	Flex/Ext	Int/Ext	Ad/Ab	Flex/Ext	Int/Ext	Ad/Ab
0.00	0.8366	0.8255	0.3604	0.1262	0.1816	0.4652	0.0027	0.0791	0.9239
0.67	0.8000	0.6943	0.2958	0.2082	0.1261	0.4206	0.0063	0.0501	0.7957
1.33	0.9126	0.6037	0.2001	0.1613	0.1217	0.4726	0.0049	0.0579	0.7295
2.00	0.9345	0.6451	0.1369	0.1285	0.1172	0.5725	0.0053	0.0978	0.7081
2.67	0.9405	0.8625	0.1031	0.1044	0.1268	0.7132	0.0068	0.2043	0.7884
3.33	0.9745	0.8393	0.0851	0.0790	0.1525	0.9140	0.0052	0.4320	0.9950
4.00	0.9529	0.5518	0.0795	0.0602	0.1800	0.8777	0.0046	0.7562	0.7504
4.67	0.8444	0.3557	0.0696	0.0404	0.2154	0.6604	0.0057	0.9370	0.4719
5.33	0.7996	0.2469	0.0612	0.0309	0.2030	0.4687	0.0062	0.7922	0.2700
6.00	0.7847	0.2043	0.0538	0.0237	0.1628	0.3543	0.0045	0.8288	0.1711
6.67	0.7476	0.2168	0.0578	0.0258	0.1081	0.3100	0.0033	0.9889	0.1593
7.33	0.7136	0.2559	0.0677	0.0263	0.0656	0.3339	0.0040	0.7385	0.2039
8.00	0.6175	0.2777	0.0713	0.0271	0.0378	0.3951	0.0045	0.5037	0.2863
8.67	0.5372	0.2851	0.0832	0.0263	0.0241	0.4757	0.0042	0.3450	0.3623
9.33	0.4902	0.2967	0.1025	0.0259	0.0161	0.5553	0.0030	0.2849	0.4512
10.00	0.4605	0.3022	0.1302	0.0241	0.0120	0.6525	0.0019	0.2787	0.5810
10.67	0.4117	0.3498	0.1503	0.0218	0.0094	0.7461	0.0014	0.2886	0.7546
11.33	0.3486	0.4257	0.1697	0.0154	0.0074	0.8030	0.0010	0.2890	0.9258
12.00	0.2789	0.5009	0.1968	0.0118	0.0048	0.8326	0.0007	0.2463	0.9548
12.67	0.2390	0.5389	0.2193	0.0102	0.0025	0.8241	0.0005	0.1833	0.8679
13.33	0.2101	0.5564	0.2469	0.0079	0.0012	0.8274	0.0004	0.1255	0.8287
14.00	0.1858	0.5832	0.2771	0.0057	0.0005	0.8324	0.0003	0.0858	0.8093
14.67	0.1718	0.5846	0.3198	0.0041	0.0003	0.8293	0.0003	0.0643	0.8146
15.33	0.1630	0.5604	0.3521	0.0037	0.0002	0.8108	0.0003	0.0539	0.8301
16.00	0.1555	0.5088	0.3887	0.0038	0.0001	0.7909	0.0003	0.0462	0.8510
16.67	0.1475	0.4416	0.4287	0.0039	0.0001	0.7750	0.0003	0.0409	0.8514
17.33	0.1553	0.3678	0.4696	0.0043	0.0001	0.7498	0.0004	0.0362	0.8399
18.00	0.1608	0.3067	0.4902	0.0048	0.0001	0.7117	0.0004	0.0317	0.8413
18.67	0.1722	0.2602	0.5143	0.0052	0.0001	0.6936	0.0004	0.0268	0.8381
19.33	0.1934	0.2193	0.5351	0.0051	0.0001	0.6670	0.0004	0.0215	0.8507
20.00	0.2318	0.1870	0.5526	0.0051	0.0002	0.6263	0.0003	0.0173	0.8591
20.67	0.2491	0.1687	0.5646	0.0045	0.0002	0.5692	0.0002	0.0128	0.8820
21.33	0.2568	0.1521	0.5693	0.0040	0.0002	0.5226	0.0002	0.0092	0.9154
22.00	0.2649	0.1316	0.5740	0.0033	0.0003	0.4862	0.0001	0.0071	0.9630

22.67	0.2754	0.1049	0.5682	0.0025	0.0003	0.4438	0.0001	0.0062	0.9557
23.33	0.2878	0.0812	0.5749	0.0017	0.0003	0.3965	0.0001	0.0050	0.8557
24.00	0.2916	0.0640	0.6069	0.0011	0.0002	0.3466	0.0001	0.0041	0.7409
24.67	0.3048	0.0539	0.6466	0.0007	0.0001	0.3074	0.0000	0.0034	0.6564
25.33	0.3092	0.0465	0.6772	0.0005	0.0001	0.2851	0.0000	0.0029	0.5972
26.00	0.3133	0.0428	0.7082	0.0004	0.0001	0.2846	0.0000	0.0026	0.5548
26.67	0.3267	0.0384	0.7262	0.0003	0.0000	0.2902	0.0000	0.0029	0.5260
27.33	0.3365	0.0352	0.7474	0.0002	0.0000	0.2924	0.0000	0.0032	0.4953
28.00	0.3333	0.0344	0.7809	0.0002	0.0000	0.3002	0.0000	0.0036	0.4863
28.67	0.3295	0.0363	0.8233	0.0003	0.0000	0.3311	0.0001	0.0041	0.5125
29.33	0.3285	0.0407	0.8321	0.0003	0.0000	0.3672	0.0001	0.0048	0.5662
30.00	0.3304	0.0453	0.8438	0.0004	0.0000	0.3912	0.0001	0.0061	0.6147
30.67	0.3387	0.0549	0.8648	0.0004	0.0000	0.4095	0.0001	0.0077	0.6432
31.33	0.3577	0.0663	0.8867	0.0005	0.0000	0.4207	0.0001	0.0089	0.6562
32.00	0.3772	0.0811	0.9033	0.0006	0.0000	0.4305	0.0001	0.0092	0.6881
32.67	0.3860	0.0925	0.9242	0.0006	0.0000	0.4382	0.0001	0.0086	0.7281
33.33	0.3932	0.1035	0.9633	0.0007	0.0000	0.4410	0.0001	0.0078	0.7479
34.00	0.4156	0.1138	0.9952	0.0009	0.0000	0.4389	0.0002	0.0069	0.7665
34.67	0.4527	0.1251	0.9690	0.0011	0.0000	0.4254	0.0002	0.0061	0.7730
35.33	0.5069	0.1227	0.9734	0.0014	0.0000	0.4129	0.0002	0.0059	0.7616
36.00	0.5801	0.1120	0.9989	0.0017	0.0000	0.4085	0.0004	0.0061	0.7673
36.67	0.6657	0.1023	0.9635	0.0020	0.0000	0.3943	0.0006	0.0062	0.7668
37.33	0.7394	0.0963	0.9482	0.0025	0.0000	0.3628	0.0010	0.0064	0.7441
38.00	0.8017	0.0938	0.9302	0.0038	0.0000	0.3336	0.0017	0.0062	0.7204
38.67	0.8751	0.0879	0.8867	0.0055	0.0000	0.3023	0.0034	0.0057	0.6913
39.33	0.9494	0.0797	0.8419	0.0083	0.0000	0.2744	0.0061	0.0052	0.6544
40.00	0.9636	0.0718	0.8017	0.0130	0.0000	0.2573	0.0089	0.0046	0.5988
40.67	0.9009	0.0646	0.7701	0.0196	0.0000	0.2499	0.0117	0.0043	0.5605
41.33	0.8453	0.0546	0.7225	0.0292	0.0000	0.2463	0.0173	0.0047	0.5381
42.00	0.8091	0.0456	0.6687	0.0445	0.0000	0.2489	0.0246	0.0060	0.5377
42.67	0.8153	0.0382	0.6295	0.0666	0.0000	0.2633	0.0316	0.0083	0.5492
43.33	0.7991	0.0309	0.6085	0.0960	0.0000	0.2751	0.0361	0.0120	0.5529
44.00	0.7925	0.0236	0.5924	0.1268	0.0000	0.2941	0.0369	0.0176	0.5492
44.67	0.7534	0.0192	0.5540	0.1737	0.0001	0.3282	0.0369	0.0242	0.5319
45.33	0.7478	0.0178	0.5169	0.2342	0.0001	0.3658	0.0426	0.0296	0.5157
46.00	0.7389	0.0211	0.4829	0.2977	0.0002	0.3840	0.0494	0.0332	0.4975
46.67	0.7354	0.0273	0.4458	0.3678	0.0004	0.3997	0.0595	0.0383	0.4958
47.33	0.7103	0.0344	0.4067	0.4641	0.0007	0.4077	0.0709	0.0470	0.5102
48.00	0.6607	0.0437	0.3651	0.5911	0.0009	0.4242	0.0748	0.0605	0.5207
48.67	0.6085	0.0547	0.3331	0.7156	0.0011	0.4432	0.0749	0.0716	0.5187
49.33	0.5843	0.0632	0.3172	0.8318	0.0012	0.4571	0.0763	0.0765	0.5274
50.00	0.5765	0.0712	0.3260	0.9520	0.0017	0.4738	0.0810	0.0759	0.5560
50.67	0.5661	0.0796	0.3368	0.9443	0.0023	0.4807	0.0827	0.0752	0.6003

51.33	0.5535	0.0810	0.3412	0.8497	0.0030	0.4833	0.0751	0.0766	0.6309
52.00	0.5476	0.0728	0.3557	0.7686	0.0032	0.5079	0.0686	0.0764	0.6465
52.67	0.5507	0.0605	0.3700	0.6878	0.0037	0.5463	0.0632	0.0749	0.6416
53.33	0.5691	0.0530	0.3954	0.6074	0.0046	0.5836	0.0502	0.0810	0.6419
54.00	0.5993	0.0456	0.4295	0.5528	0.0058	0.6115	0.0378	0.1022	0.6359
54.67	0.6403	0.0408	0.4784	0.5317	0.0083	0.6155	0.0252	0.1322	0.6230
55.33	0.7013	0.0373	0.5195	0.5352	0.0095	0.6012	0.0160	0.1606	0.5780
56.00	0.7757	0.0350	0.5559	0.5396	0.0106	0.5979	0.0104	0.1744	0.5424
56.67	0.8514	0.0337	0.5943	0.5500	0.0126	0.6052	0.0063	0.1700	0.5237
57.33	0.9181	0.0336	0.6287	0.5681	0.0120	0.6108	0.0035	0.1571	0.5250
58.00	0.9742	0.0387	0.6494	0.6149	0.0097	0.6069	0.0019	0.1495	0.5314
58.67	0.9820	0.0450	0.6932	0.6860	0.0077	0.5924	0.0010	0.1346	0.5355
59.33	0.9204	0.0659	0.7664	0.7347	0.0055	0.5774	0.0006	0.1081	0.5305
60.00	0.8901	0.0961	0.8165	0.7944	0.0036	0.5486	0.0003	0.0833	0.5273
60.67	0.8628	0.1256	0.8122	0.9021	0.0029	0.4873	0.0002	0.0687	0.5234
61.33	0.8542	0.1415	0.7824	0.9562	0.0027	0.4109	0.0001	0.0537	0.5042
62.00	0.7859	0.1526	0.7864	0.8287	0.0021	0.3484	0.0001	0.0413	0.5008
62.67	0.7661	0.1559	0.8156	0.7375	0.0012	0.3037	0.0000	0.0331	0.5044
63.33	0.7035	0.1766	0.8594	0.6568	0.0006	0.2798	0.0000	0.0255	0.4999
64.00	0.6822	0.1934	0.8704	0.5795	0.0002	0.2599	0.0000	0.0177	0.4780
64.67	0.6341	0.2164	0.8685	0.5002	0.0001	0.2304	0.0000	0.0133	0.4488
65.33	0.6197	0.2305	0.8459	0.4671	0.0000	0.2083	0.0000	0.0119	0.4291
66.00	0.5737	0.2470	0.8097	0.4445	0.0000	0.1980	0.0000	0.0121	0.4536
66.67	0.5377	0.2955	0.7695	0.4234	0.0000	0.2069	0.0000	0.0129	0.5008
67.33	0.5070	0.3563	0.7562	0.4045	0.0000	0.2107	0.0000	0.0153	0.5381
68.00	0.4926	0.3948	0.7700	0.3802	0.0000	0.1866	0.0000	0.0190	0.5240
68.67	0.4780	0.3948	0.8036	0.3595	0.0000	0.1626	0.0000	0.0203	0.5102
69.33	0.4582	0.4081	0.8304	0.3232	0.0000	0.1465	0.0000	0.0200	0.5165
70.00	0.4457	0.4568	0.8167	0.2753	0.0000	0.1464	0.0000	0.0217	0.5481
70.67	0.4253	0.5319	0.7879	0.2466	0.0000	0.1604	0.0000	0.0233	0.6031
71.33	0.3995	0.6121	0.8053	0.2246	0.0000	0.1801	0.0001	0.0230	0.6512
72.00	0.3646	0.6523	0.8463	0.2054	0.0000	0.2087	0.0001	0.0232	0.7009
72.67	0.3320	0.6859	0.8596	0.1631	0.0000	0.2636	0.0003	0.0258	0.7389
73.33	0.2928	0.6941	0.8080	0.1285	0.0000	0.3192	0.0005	0.0351	0.7786
74.00	0.2320	0.6741	0.7344	0.0998	0.0000	0.3680	0.0009	0.0521	0.8253
74.67	0.1772	0.6188	0.6653	0.0798	0.0000	0.4246	0.0013	0.0843	0.9116
75.33	0.1416	0.5441	0.6095	0.0553	0.0000	0.4935	0.0014	0.1408	0.9928
76.00	0.1282	0.4763	0.5803	0.0352	0.0000	0.5738	0.0014	0.2214	0.9289
76.67	0.1113	0.4195	0.5784	0.0196	0.0000	0.5864	0.0011	0.2892	0.9081
77.33	0.0973	0.3628	0.6011	0.0105	0.0000	0.5530	0.0009	0.3293	0.9115
78.00	0.0928	0.3225	0.6122	0.0052	0.0000	0.5332	0.0007	0.3277	0.9580
78.67	0.0991	0.2966	0.6073	0.0025	0.0000	0.5098	0.0005	0.3066	0.9910
79.33	0.1090	0.2762	0.5910	0.0013	0.0000	0.4848	0.0004	0.2700	0.9663

80.00	0.1247	0.2617	0.5897	0.0007	0.0000	0.4534	0.0004	0.2358	0.9622
80.67	0.1471	0.2489	0.6082	0.0004	0.0000	0.4301	0.0004	0.2082	0.9579
81.33	0.1820	0.2443	0.6356	0.0003	0.0000	0.4058	0.0006	0.1970	0.9521
82.00	0.2161	0.2401	0.6619	0.0003	0.0000	0.3984	0.0008	0.2005	0.9446
82.67	0.2350	0.2597	0.6842	0.0004	0.0000	0.3968	0.0014	0.2032	0.9368
83.33	0.2609	0.2912	0.7286	0.0006	0.0000	0.3776	0.0030	0.1936	0.9278
84.00	0.2920	0.3083	0.7858	0.0011	0.0000	0.3511	0.0070	0.1700	0.8946
84.67	0.3282	0.2978	0.8128	0.0024	0.0001	0.3389	0.0159	0.1427	0.8354
85.33	0.3760	0.2705	0.8104	0.0065	0.0001	0.3420	0.0374	0.1149	0.7973
86.00	0.4337	0.2505	0.7777	0.0179	0.0001	0.3653	0.0759	0.0929	0.7850
86.67	0.4857	0.2428	0.7398	0.0449	0.0001	0.3909	0.1393	0.0777	0.7909
87.33	0.5073	0.2597	0.7145	0.0969	0.0001	0.4024	0.2300	0.0742	0.8421
88.00	0.5389	0.2553	0.6742	0.1938	0.0002	0.3897	0.3553	0.0763	0.9249
88.67	0.5831	0.2231	0.6079	0.3263	0.0005	0.3853	0.4926	0.0863	0.9889
89.33	0.6425	0.1561	0.4881	0.4663	0.0010	0.3851	0.6156	0.0956	0.9938
90.00	0.6329	0.0965	0.3641	0.6067	0.0016	0.3717	0.6798	0.0987	0.9711
90.67	0.6219	0.0534	0.2756	0.7354	0.0019	0.3619	0.6968	0.0866	0.9021
91.33	0.6232	0.0273	0.2354	0.8274	0.0021	0.3663	0.6813	0.0785	0.8033
92.00	0.6564	0.0170	0.2172	0.9085	0.0024	0.3906	0.7213	0.0783	0.7042
92.67	0.6477	0.0150	0.2230	0.9397	0.0020	0.4038	0.7194	0.0803	0.5871
93.33	0.6155	0.0144	0.2352	0.9338	0.0012	0.4062	0.6627	0.0982	0.5292
94.00	0.5797	0.0146	0.2406	0.8617	0.0006	0.4083	0.5391	0.1150	0.5006
94.67	0.6705	0.0202	0.2502	0.7728	0.0005	0.3978	0.3776	0.1475	0.5317
95.33	0.7375	0.0331	0.2437	0.6648	0.0005	0.3927	0.2767	0.1720	0.5908
96.00	0.7884	0.0545	0.2445	0.5383	0.0010	0.3964	0.1998	0.1963	0.6487
96.67	0.7917	0.0818	0.2340	0.4599	0.0027	0.3885	0.1190	0.1466	0.6411
97.33	0.8519	0.1227	0.2090	0.3715	0.0074	0.3921	0.0591	0.1099	0.6449
98.00	0.9918	0.1685	0.1633	0.2832	0.0170	0.3985	0.0233	0.0813	0.6614
98.67	0.9219	0.2054	0.1193	0.1988	0.0385	0.4043	0.0108	0.0588	0.7119
99.33	0.8599	0.1977	0.0918	0.1582	0.0844	0.4334	0.0062	0.0402	0.7701
100.00	0.7856	0.1807	0.1098	0.1536	0.1659	0.4998	0.0034	0.0295	0.7783

Table 4. Summary of p-values for flexion-extension, internal-external, and abduction-adduction rotation angles during step up and over task for bilateral control (LR), ACLd, and PFP populations.

Bilateral Differences in Healthy Control Group

During the step-up and over task significant differences ($p<0.05$) were observed for internal-external rotation between 26-31%, 42-48%, 54-59%, and 92-96% of the cycle. No other differences were observed between bilateral control subjects during step up and over.

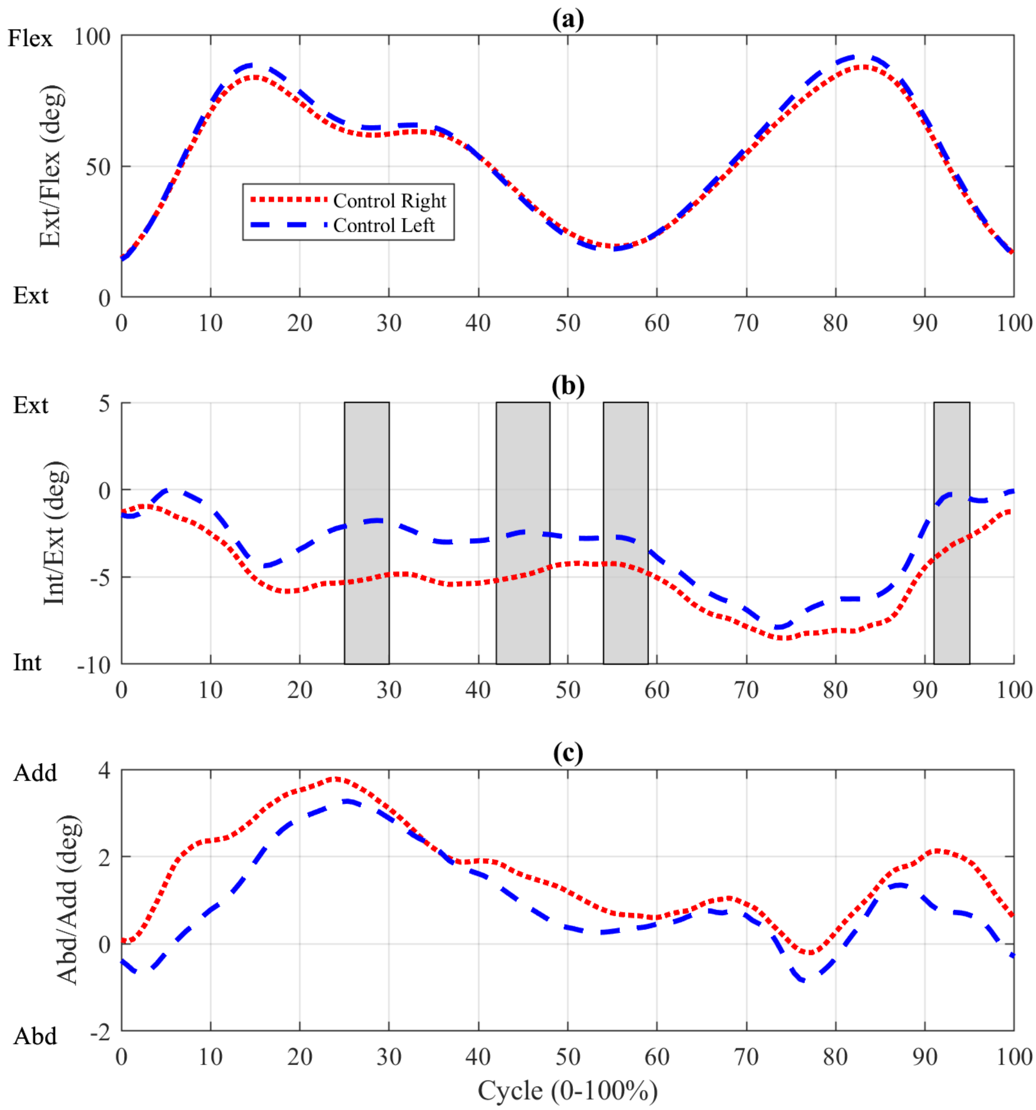

Figure 4. Rotation angles during step-up and over for bilateral control group. (a) Flexion-extension. (b) Internal-external. Significantly less left internal rotation between 26-31%, 42-48%, 54-59%, and 92-96% of the cycle. (c) Varus-valgus. Shaded regions indicate areas of significant differences.

ACLd Group

For the step up and over task, more external rotation was observed between 8-99% of the cycle and flexion-extension angles were significantly different between 5-42% and 76-87% of the cycle.

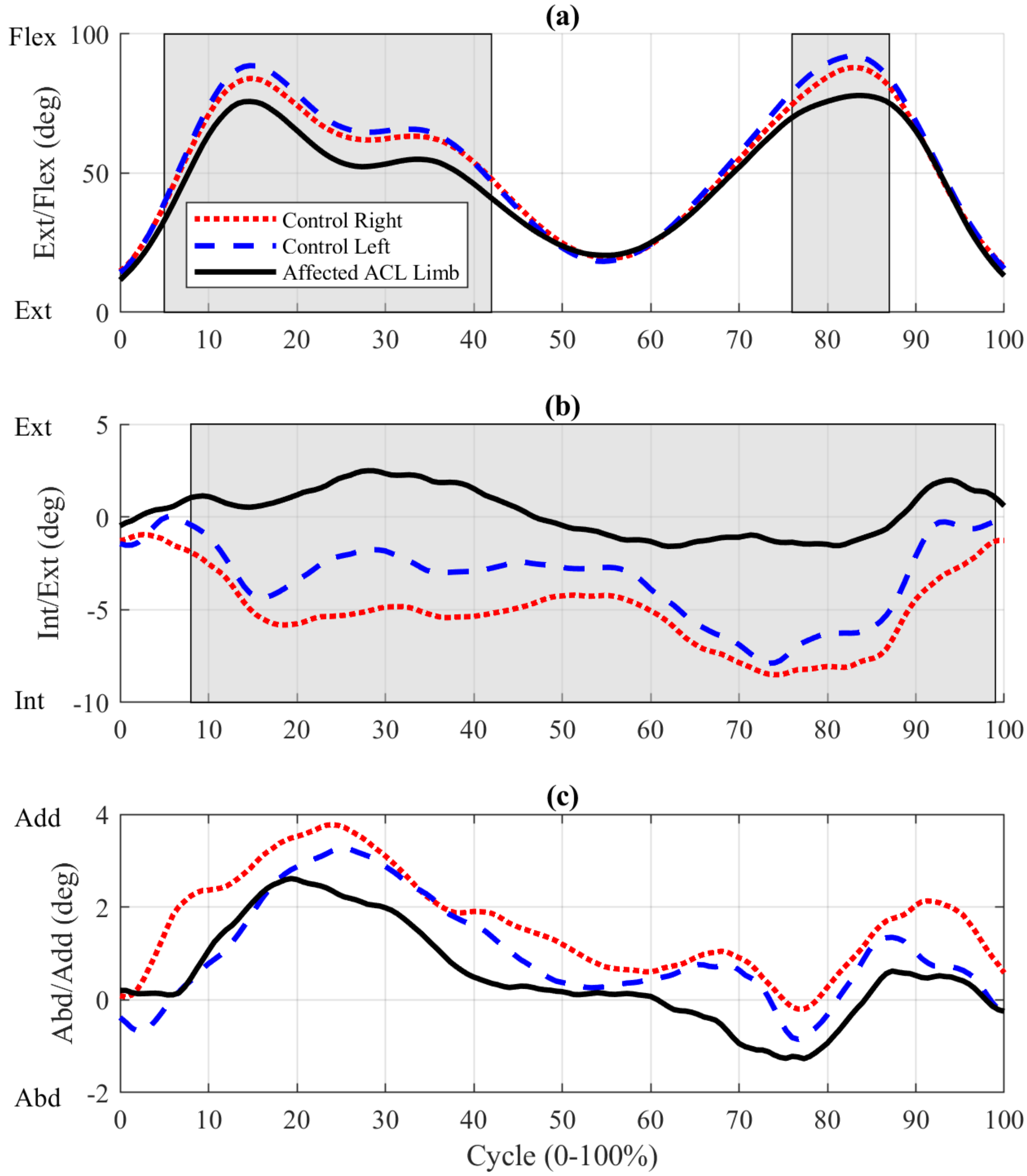

Figure 5. Rotation angles during step-up and over for ACLd group. (a) Flexion-extension. Significantly lower ACLd flexion rotation between 5-42% and 76-87% (b) Internal-external. Significantly more ACLd external rotation between 8-99% of the cycle. (c) Varus-valgus. Shaded regions indicate areas of significant differences.

PFP Group

Comparison of cycle normalized ensemble averages showed statistically significant differences ($p<0.05$) in internal-external rotation between PFP and healthy control group for 42% of the cycle during step-up and over tasks and 30% of the cycle for lateral step-down tasks. Flexion-extension rotation had significant differences for 76% of step-up and over tasks and 99% of lateral step-down tasks.

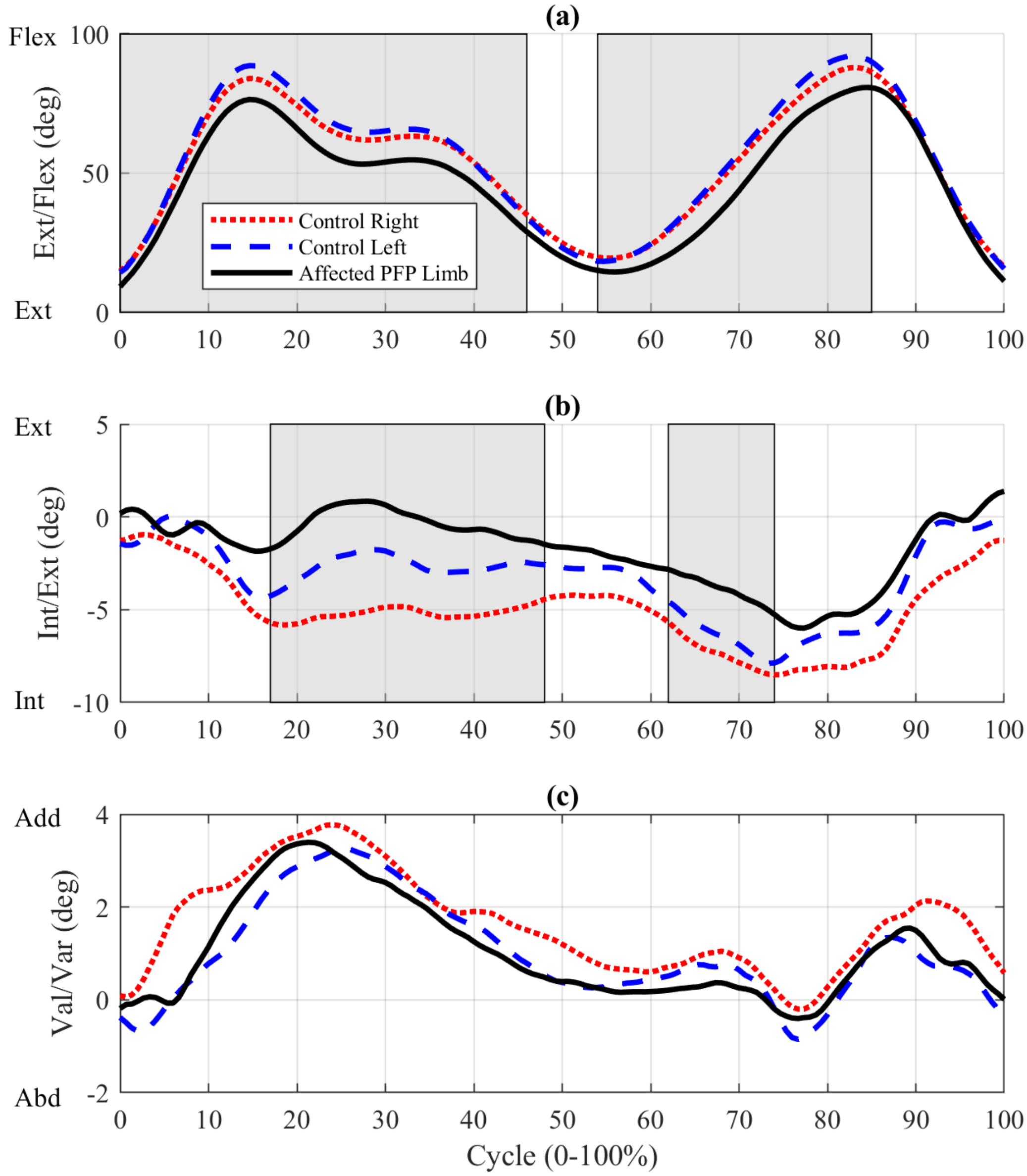

Figure 6. Rotation angles during step-up and over for PFP group. (a) Flexion-extension. Significantly lower PFP flexion rotation between 0-46% and 54-85% (b) Internal-external. Significantly less PFP internal rotation between 17-48% and 62-74% of the cycle. (c) Varus-valgus. Shaded regions indicate areas of significant differences.

4.1.3 Lateral Step Down

Table 5 summarizes the p-values during the lateral step-down task for all participant groups.

	LR			**ACLd**			**PFP**		
% of Cycle	Flex/Ext	Int/Ext	Ad/Ab	Flex/Ext	Int/Ext	Ad/Ab	Flex/Ext	Int/Ext	Ad/Ab
0	0.3901	0.8222	0.1508	0.5689	0.0166	0.0879	0.0858	0.0411	0.9351
1	0.3775	0.7646	0.1572	0.5213	0.0122	0.1011	0.0671	0.0313	0.9653
2	0.3686	0.7376	0.1401	0.5133	0.0098	0.1217	0.0635	0.0292	0.9114
3	0.3639	0.7004	0.1324	0.5305	0.0079	0.1417	0.0569	0.0272	0.8664
4	0.3698	0.6908	0.1428	0.5741	0.0063	0.1646	0.0501	0.0233	0.8008
5	0.3672	0.7204	0.1713	0.6482	0.0054	0.1912	0.0402	0.0197	0.7305
6	0.3859	0.7450	0.2008	0.7342	0.0046	0.2092	0.0314	0.0188	0.6828
7	0.4200	0.7583	0.2278	0.8129	0.0038	0.2072	0.0230	0.0184	0.6743
8	0.4646	0.7719	0.2729	0.9126	0.0033	0.2047	0.0197	0.0167	0.6753
9	0.4887	0.8436	0.3227	0.9642	0.0029	0.1963	0.0174	0.0151	0.6681
10	0.5414	0.9021	0.3576	0.8468	0.0026	0.1812	0.0161	0.0143	0.6644
11	0.5909	0.9503	0.3759	0.7366	0.0022	0.1603	0.0150	0.0140	0.7062
12	0.6709	0.9840	0.4098	0.6386	0.0019	0.1384	0.0129	0.0144	0.7632
13	0.7581	0.9808	0.4428	0.5273	0.0016	0.1159	0.0127	0.0152	0.8282
14	0.8043	0.9067	0.4487	0.4235	0.0014	0.0995	0.0154	0.0159	0.9038
15	0.8557	0.8341	0.4236	0.3307	0.0011	0.0889	0.0173	0.0181	0.9758
16	0.8953	0.7775	0.3991	0.2763	0.0008	0.0855	0.0170	0.0213	0.9675
17	0.9579	0.7686	0.3894	0.2288	0.0005	0.0829	0.0163	0.0247	0.8964
18	0.9999	0.8054	0.3843	0.1910	0.0003	0.0795	0.0176	0.0249	0.8276
19	0.9385	0.8550	0.3911	0.1450	0.0002	0.0719	0.0169	0.0216	0.7810
20	0.8558	0.8958	0.4081	0.1107	0.0002	0.0657	0.0175	0.0187	0.7541
21	0.7843	0.9218	0.4280	0.0845	0.0001	0.0616	0.0179	0.0169	0.7325
22	0.7542	0.9051	0.4305	0.0684	0.0001	0.0602	0.0179	0.0175	0.6878
23	0.7457	0.9242	0.4283	0.0532	0.0001	0.0620	0.0165	0.0217	0.6369
24	0.7258	0.9876	0.4426	0.0409	0.0001	0.0648	0.0161	0.0270	0.6120
25	0.6846	0.9495	0.4847	0.0308	0.0001	0.0662	0.0159	0.0304	0.5909
26	0.6437	0.9202	0.5315	0.0244	0.0001	0.0657	0.0158	0.0301	0.5715
27	0.6108	0.9022	0.5492	0.0184	0.0001	0.0657	0.0150	0.0294	0.5669
28	0.6159	0.8845	0.5477	0.0143	0.0000	0.0691	0.0154	0.0308	0.5849
29	0.6092	0.8530	0.5611	0.0112	0.0000	0.0749	0.0168	0.0350	0.6072
30	0.5983	0.8054	0.5832	0.0096	0.0000	0.0778	0.0175	0.0374	0.6030
31	0.5862	0.7561	0.6199	0.0083	0.0000	0.0789	0.0179	0.0390	0.5861
32	0.5678	0.7192	0.6717	0.0070	0.0000	0.0804	0.0169	0.0406	0.5813

33	0.5615	0.7100	0.7005	0.0057	0.0000	0.0819	0.0162	0.0466	0.5936
34	0.5469	0.7035	0.7063	0.0048	0.0000	0.0855	0.0156	0.0517	0.5965
35	0.5168	0.6854	0.7058	0.0045	0.0000	0.0908	0.0155	0.0554	0.5933
36	0.4871	0.6662	0.7223	0.0041	0.0000	0.0973	0.0152	0.0587	0.5958
37	0.4599	0.6473	0.7377	0.0036	0.0000	0.1013	0.0136	0.0632	0.6053
38	0.4475	0.6368	0.7406	0.0034	0.0000	0.1069	0.0122	0.0681	0.6170
39	0.4302	0.6269	0.7383	0.0033	0.0000	0.1145	0.0116	0.0739	0.6318
40	0.4079	0.6206	0.7531	0.0033	0.0000	0.1220	0.0112	0.0805	0.6384
41	0.3842	0.6207	0.7807	0.0031	0.0000	0.1272	0.0103	0.0888	0.6376
42	0.3651	0.6225	0.8044	0.0031	0.0000	0.1344	0.0097	0.0928	0.6351
43	0.3475	0.6157	0.8282	0.0030	0.0000	0.1408	0.0089	0.0931	0.6370
44	0.3361	0.6048	0.8596	0.0029	0.0000	0.1437	0.0082	0.0914	0.6468
45	0.3316	0.5970	0.8750	0.0026	0.0000	0.1450	0.0075	0.0933	0.6599
46	0.3255	0.5841	0.8804	0.0023	0.0000	0.1460	0.0066	0.0981	0.6778
47	0.3164	0.5754	0.8775	0.0022	0.0001	0.1480	0.0061	0.1020	0.6959
48	0.3065	0.5696	0.8650	0.0021	0.0001	0.1543	0.0056	0.1047	0.7145
49	0.3100	0.5580	0.8638	0.0020	0.0001	0.1609	0.0052	0.1078	0.7341
50	0.3071	0.5382	0.8706	0.0019	0.0001	0.1679	0.0047	0.1127	0.7576
51	0.3025	0.5167	0.8854	0.0018	0.0001	0.1742	0.0042	0.1199	0.7862
52	0.2978	0.5021	0.8977	0.0018	0.0001	0.1838	0.0038	0.1290	0.8225
53	0.2950	0.4950	0.9096	0.0018	0.0002	0.1950	0.0034	0.1376	0.8542
54	0.2926	0.4813	0.9197	0.0018	0.0002	0.2001	0.0032	0.1449	0.8761
55	0.2886	0.4730	0.9235	0.0019	0.0002	0.1992	0.0030	0.1522	0.8986
56	0.2834	0.4683	0.9285	0.0020	0.0002	0.1986	0.0028	0.1596	0.9185
57	0.2807	0.4682	0.9357	0.0020	0.0002	0.2002	0.0027	0.1667	0.9430
58	0.2726	0.4739	0.9446	0.0019	0.0002	0.1991	0.0027	0.1747	0.9643
59	0.2683	0.4859	0.9518	0.0016	0.0002	0.1976	0.0027	0.1810	0.9884
60	0.2602	0.4936	0.9500	0.0013	0.0002	0.1958	0.0027	0.1919	0.9961
61	0.2521	0.4973	0.9400	0.0011	0.0002	0.1901	0.0028	0.2039	0.9809
62	0.2458	0.5011	0.9188	0.0009	0.0002	0.1879	0.0031	0.2147	0.9751
63	0.2455	0.4973	0.8927	0.0007	0.0002	0.1878	0.0035	0.2185	0.9791
64	0.2505	0.4829	0.8736	0.0006	0.0002	0.1897	0.0038	0.2183	0.9771
65	0.2632	0.4691	0.8480	0.0006	0.0002	0.1920	0.0042	0.2141	0.9633
66	0.2732	0.4607	0.8111	0.0006	0.0002	0.1930	0.0046	0.2030	0.9486
67	0.2865	0.4548	0.7813	0.0006	0.0002	0.1895	0.0053	0.1909	0.9470
68	0.2979	0.4434	0.7708	0.0006	0.0002	0.1825	0.0062	0.1847	0.9547
69	0.3270	0.4272	0.7619	0.0006	0.0001	0.1727	0.0072	0.1824	0.9668
70	0.3550	0.4065	0.7453	0.0007	0.0001	0.1612	0.0088	0.1864	0.9820
71	0.3705	0.3765	0.7327	0.0009	0.0001	0.1537	0.0108	0.1949	0.9982
72	0.3910	0.3310	0.7288	0.0010	0.0002	0.1483	0.0124	0.2125	0.9780
73	0.4132	0.2934	0.7319	0.0012	0.0002	0.1437	0.0126	0.2313	0.9636
74	0.4389	0.2587	0.7250	0.0015	0.0003	0.1436	0.0118	0.2570	0.9635
75	0.4567	0.2359	0.7070	0.0023	0.0004	0.1464	0.0120	0.2768	0.9956

76	0.4810	0.2238	0.6896	0.0032	0.0006	0.1518	0.0136	0.2881	0.9632
77	0.5079	0.2284	0.6699	0.0043	0.0008	0.1523	0.0135	0.2979	0.9394
78	0.5387	0.2284	0.6449	0.0060	0.0011	0.1548	0.0129	0.3156	0.9242
79	0.5868	0.2235	0.6181	0.0093	0.0014	0.1579	0.0124	0.3333	0.9129
80	0.6368	0.2303	0.5905	0.0133	0.0016	0.1620	0.0123	0.3436	0.8893
81	0.6839	0.2396	0.5782	0.0198	0.0019	0.1684	0.0126	0.3451	0.8603
82	0.6925	0.2477	0.5694	0.0282	0.0023	0.1765	0.0142	0.3479	0.8342
83	0.7356	0.2638	0.5217	0.0464	0.0028	0.1809	0.0162	0.3480	0.8093
84	0.8133	0.2742	0.4495	0.0730	0.0035	0.1864	0.0177	0.3391	0.7930
85	0.8855	0.2872	0.3903	0.1035	0.0041	0.1892	0.0199	0.3142	0.7865
86	0.9531	0.3130	0.3380	0.1427	0.0044	0.1941	0.0220	0.2718	0.7560
87	0.9662	0.3462	0.3049	0.2018	0.0049	0.2028	0.0236	0.2325	0.7304
88	0.9100	0.3829	0.2759	0.2829	0.0057	0.2085	0.0258	0.1950	0.7130
89	0.8044	0.4330	0.2428	0.3961	0.0061	0.2125	0.0289	0.1589	0.6987
90	0.7481	0.4789	0.2193	0.5112	0.0064	0.2157	0.0324	0.1350	0.6807
91	0.7476	0.5147	0.2072	0.6377	0.0067	0.2206	0.0387	0.1196	0.6532
92	0.6986	0.5598	0.2141	0.7678	0.0070	0.2159	0.0437	0.0999	0.6416
93	0.6424	0.6237	0.2233	0.9007	0.0073	0.2005	0.0468	0.0875	0.6544
94	0.5821	0.7076	0.2392	0.9971	0.0070	0.1807	0.0441	0.0781	0.6726
95	0.5204	0.8121	0.2507	0.8995	0.0071	0.1665	0.0454	0.0723	0.6719
96	0.4949	0.9188	0.2560	0.8191	0.0078	0.1543	0.0481	0.0694	0.6748
97	0.4755	0.9494	0.2451	0.7077	0.0083	0.1370	0.0493	0.0627	0.7080
98	0.4397	0.9280	0.2281	0.6170	0.0085	0.1173	0.0523	0.0568	0.7577
99	0.4215	0.8902	0.2112	0.5653	0.0091	0.1005	0.0528	0.0563	0.8056
100	0.3982	0.8349	0.2063	0.5266	0.0104	0.0842	0.0583	0.0583	0.8562

Table 5. Summary of p-values for flexion-extension, internal-external, and abduction-adduction rotation angles during lateral step-down task for bilateral control (LR), ACLd, and PFP populations.

ACLd Group

Data from the lateral step-down task shows an increase in external rotation for 100% of the cycle and an increase in flexion for 25-82% of the cycle. There were no significant differences in abduction-adduction rotation angles. No differences were observed between left and right control data. Most participants were able to perform the lateral step down, but in varying degrees. One ACLd participant data set was excluded for reasons mentioned in Section 4.1.

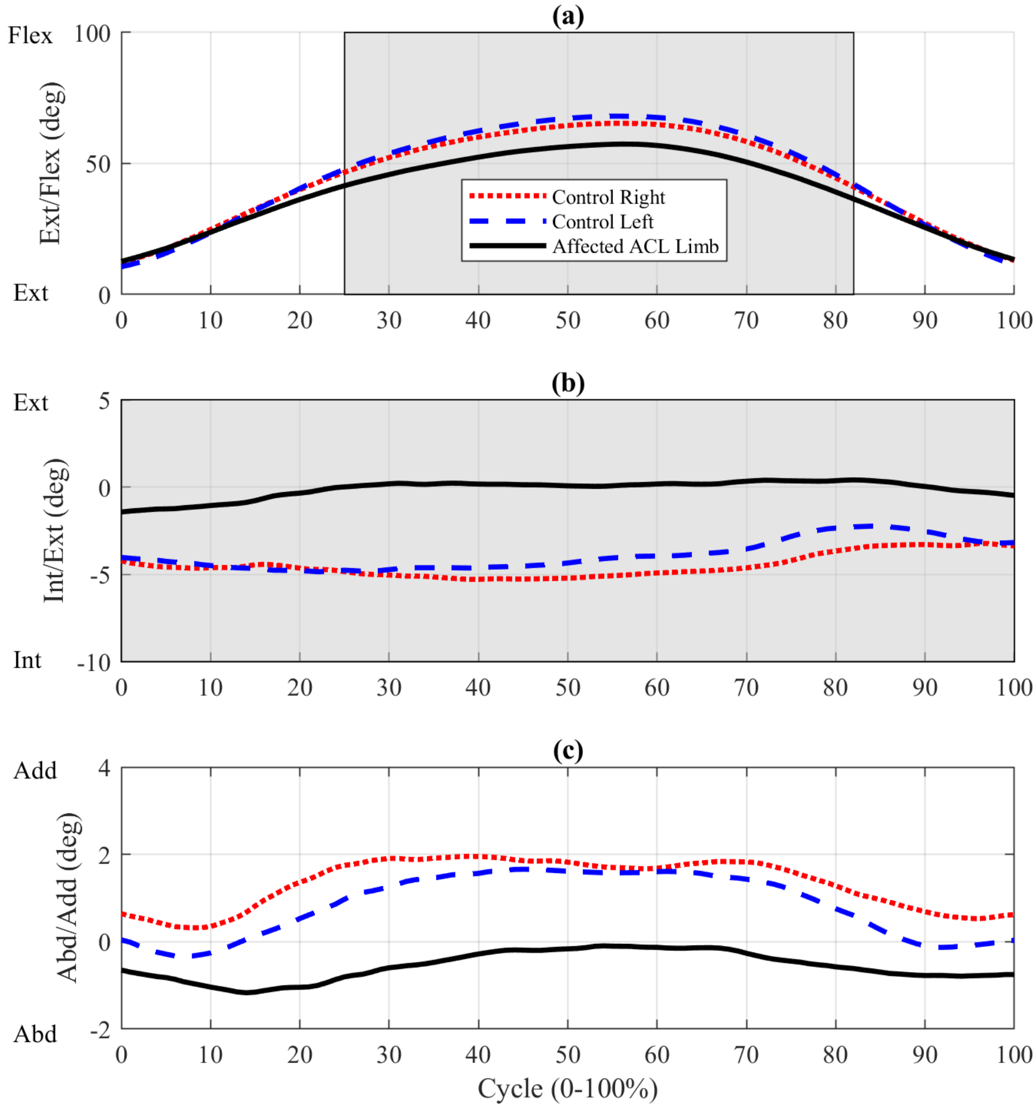

Figure 7. Rotation angles during lateral step-down for ACLd group. (a) Flexion-extension. Significantly lower ACLd flexion rotation for 25-82% of the cycle. (b) Internal-external. Significantly less ACLd internal rotation for 100% of the cycle. (c) Varus-valgus. Shaded regions indicate areas of significant differences.

PFP Population

Data from the lateral step-down task shows an increase in external rotation between 0-33% of the cycle and an increase in flexion for 5-97% of the cycle. There were no significant differences in abduction-adduction rotation angles. No differences were observed between left and right control data. Most participants were able to perform the lateral step down, but in varying degrees.

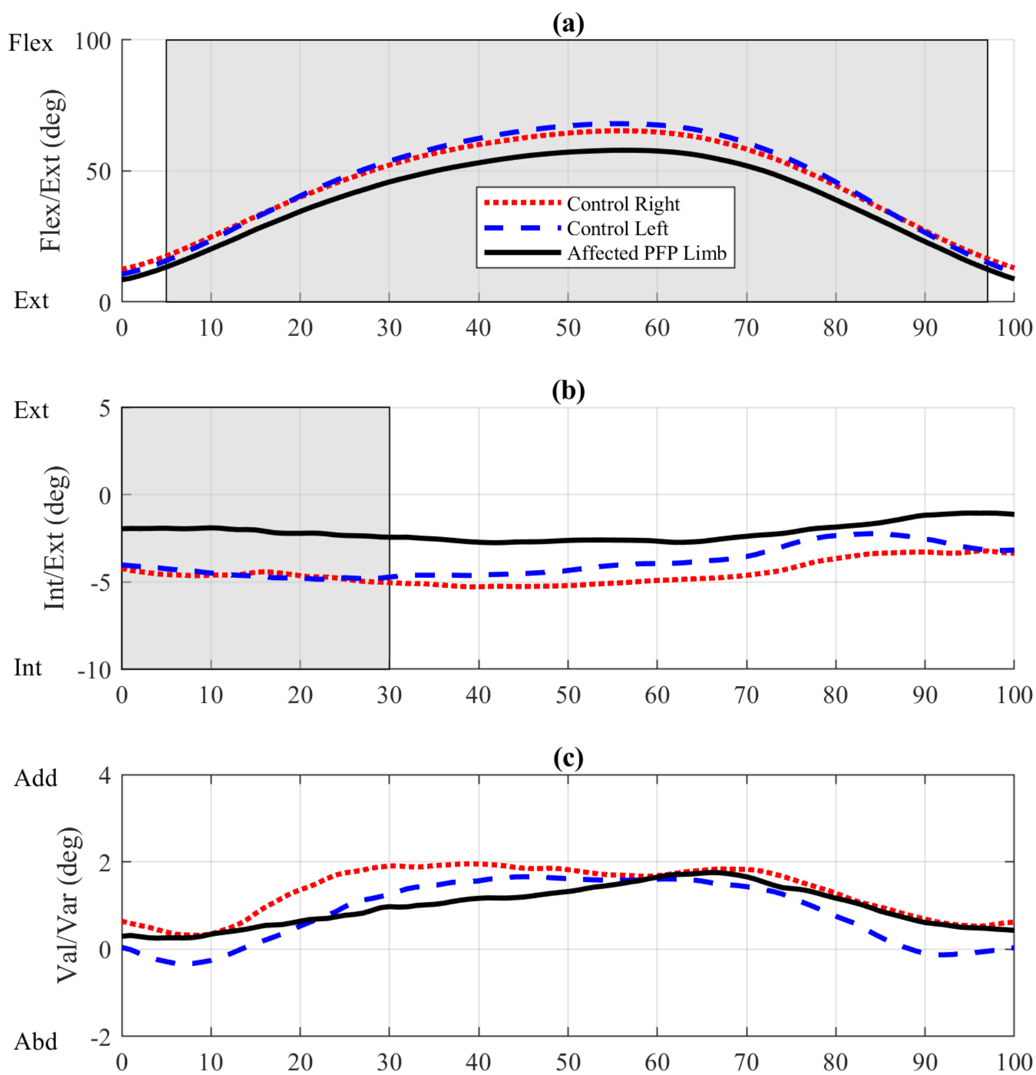

Figure 8. Rotation angles during lateral step-down for PFP group. (a) Flexion-extension. Significantly lower PFP flexion rotation between 5-97% (b) Internal-external. Significantly less PFP internal rotation between 0-33% of the cycle. (c) Varus-valgus. Shaded regions indicate areas of significant differences.

4.1.4 Y-balance (posteromedial and posterolateral)

Table 6 summarizes the p-values during the posteromedial Y-balance task for all participant groups.

	LR			**ACLd**			**PFP**		
% of Cycle	Flex/Ext	Int/Ext	Ad/Ab	Flex/Ext	Int/Ext	Ad/Ab	Flex/Ext	Int/Ext	Ad/Ab
0	0.5995	0.1550	0.0328	0.3205	0.0197	0.0719	0.0812	0.0031	0.9716
1	0.7404	0.1528	0.0309	0.3091	0.0170	0.0885	0.0851	0.0027	0.9431
2	0.7563	0.1361	0.0459	0.2763	0.0145	0.1049	0.0705	0.0026	0.9155
3	0.7473	0.1213	0.0615	0.2394	0.0126	0.1120	0.0576	0.0028	0.8982
4	0.7322	0.1166	0.0769	0.2024	0.0113	0.1144	0.0431	0.0031	0.8637
5	0.6869	0.1168	0.1032	0.1587	0.0096	0.1105	0.0301	0.0034	0.8164
6	0.6341	0.1306	0.1454	0.1185	0.0080	0.1041	0.0209	0.0039	0.7753
7	0.5873	0.1521	0.2082	0.0844	0.0066	0.1034	0.0138	0.0039	0.7545
8	0.5892	0.1689	0.2751	0.0595	0.0054	0.1081	0.0086	0.0036	0.7365
9	0.5816	0.1920	0.3555	0.0430	0.0042	0.1106	0.0044	0.0027	0.7335
10	0.5440	0.2237	0.4464	0.0304	0.0034	0.1095	0.0025	0.0021	0.7315
11	0.5211	0.2529	0.5271	0.0206	0.0026	0.1079	0.0014	0.0018	0.7421
12	0.5107	0.2519	0.5790	0.0142	0.0018	0.1083	0.0008	0.0017	0.7412
13	0.5272	0.2263	0.6237	0.0102	0.0012	0.1029	0.0004	0.0018	0.7475
14	0.5310	0.2147	0.6464	0.0079	0.0008	0.0958	0.0002	0.0020	0.7726
15	0.5077	0.2275	0.6504	0.0056	0.0007	0.0904	0.0001	0.0019	0.8361
16	0.4949	0.2573	0.6457	0.0039	0.0008	0.0861	0.0000	0.0016	0.8799
17	0.5228	0.2761	0.6259	0.0029	0.0008	0.0814	0.0000	0.0012	0.9273
18	0.5332	0.2814	0.6293	0.0021	0.0008	0.0776	0.0000	0.0010	0.9460
19	0.5224	0.2747	0.6868	0.0018	0.0007	0.0770	0.0000	0.0012	0.9473
20	0.5088	0.2942	0.7570	0.0016	0.0007	0.0758	0.0000	0.0013	0.9633
21	0.5334	0.3299	0.8069	0.0013	0.0007	0.0728	0.0000	0.0013	0.9949
22	0.5509	0.3788	0.8228	0.0011	0.0006	0.0716	0.0000	0.0010	0.9756
23	0.5454	0.3992	0.8304	0.0011	0.0005	0.0689	0.0000	0.0011	0.9292
24	0.5334	0.3895	0.8691	0.0011	0.0004	0.0680	0.0000	0.0012	0.8916
25	0.5298	0.3924	0.9029	0.0010	0.0003	0.0666	0.0000	0.0013	0.8597
26	0.5172	0.4205	0.9211	0.0010	0.0002	0.0668	0.0000	0.0012	0.8481
27	0.5259	0.4397	0.9267	0.0010	0.0002	0.0707	0.0000	0.0010	0.8838
28	0.5351	0.4573	0.9236	0.0010	0.0001	0.0732	0.0000	0.0008	0.9341
29	0.5497	0.4792	0.9370	0.0011	0.0001	0.0756	0.0000	0.0008	0.9736
30	0.5463	0.5247	0.9624	0.0011	0.0001	0.0751	0.0000	0.0008	0.9861
31	0.5578	0.5694	0.9924	0.0011	0.0001	0.0806	0.0000	0.0007	0.9938
32	0.5655	0.6080	0.9399	0.0011	0.0001	0.0886	0.0000	0.0006	0.9584

33	0.5726	0.6354	0.9051	0.0011	0.0001	0.1018	0.0000	0.0006	0.9169
34	0.5727	0.6748	0.8774	0.0012	0.0001	0.1164	0.0000	0.0006	0.8705
35	0.5766	0.7319	0.8662	0.0012	0.0001	0.1321	0.0000	0.0007	0.8305
36	0.5966	0.7727	0.8531	0.0013	0.0001	0.1481	0.0000	0.0008	0.8031
37	0.5956	0.7975	0.8382	0.0014	0.0000	0.1715	0.0000	0.0010	0.7890
38	0.5988	0.8002	0.8179	0.0015	0.0000	0.1915	0.0000	0.0012	0.7815
39	0.6001	0.8064	0.8058	0.0015	0.0001	0.2138	0.0000	0.0015	0.7697
40	0.6036	0.8107	0.7955	0.0016	0.0001	0.2312	0.0000	0.0018	0.7461
41	0.6157	0.8212	0.7923	0.0017	0.0001	0.2394	0.0000	0.0021	0.7291
42	0.6370	0.8242	0.7739	0.0018	0.0001	0.2428	0.0000	0.0022	0.7151
43	0.6532	0.8201	0.7495	0.0020	0.0001	0.2499	0.0000	0.0024	0.6963
44	0.6647	0.8123	0.7240	0.0020	0.0001	0.2553	0.0000	0.0028	0.6847
45	0.6799	0.8028	0.7194	0.0021	0.0001	0.2585	0.0000	0.0033	0.6881
46	0.6971	0.7889	0.7087	0.0021	0.0001	0.2727	0.0000	0.0039	0.6906
47	0.7162	0.7710	0.6987	0.0023	0.0001	0.2952	0.0000	0.0045	0.6769
48	0.7385	0.7529	0.6937	0.0023	0.0001	0.3134	0.0000	0.0049	0.6559
49	0.7632	0.7385	0.6826	0.0023	0.0001	0.3292	0.0000	0.0053	0.6329
50	0.7817	0.7362	0.6797	0.0023	0.0001	0.3453	0.0000	0.0057	0.6114
51	0.7965	0.7358	0.6854	0.0022	0.0001	0.3532	0.0000	0.0064	0.6043
52	0.8144	0.7334	0.6838	0.0022	0.0001	0.3580	0.0000	0.0071	0.6039
53	0.8355	0.7151	0.6791	0.0021	0.0001	0.3604	0.0000	0.0075	0.6126
54	0.8558	0.6998	0.6758	0.0020	0.0001	0.3581	0.0000	0.0080	0.6255
55	0.8681	0.6821	0.6675	0.0019	0.0001	0.3580	0.0000	0.0083	0.6349
56	0.8773	0.6636	0.6621	0.0017	0.0001	0.3599	0.0000	0.0084	0.6386
57	0.8855	0.6466	0.6613	0.0016	0.0001	0.3689	0.0000	0.0085	0.6385
58	0.8959	0.6289	0.6641	0.0015	0.0001	0.3720	0.0000	0.0089	0.6372
59	0.9141	0.6126	0.6595	0.0013	0.0001	0.3779	0.0000	0.0096	0.6300
60	0.9241	0.5933	0.6577	0.0012	0.0001	0.3843	0.0000	0.0104	0.6229
61	0.9301	0.5764	0.6569	0.0011	0.0001	0.3840	0.0000	0.0110	0.6230
62	0.9400	0.5532	0.6644	0.0010	0.0001	0.3804	0.0000	0.0117	0.6264
63	0.9602	0.5311	0.6663	0.0008	0.0001	0.3701	0.0000	0.0129	0.6304
64	0.9820	0.5060	0.6762	0.0007	0.0001	0.3606	0.0000	0.0137	0.6336
65	0.9997	0.4804	0.6953	0.0007	0.0001	0.3355	0.0000	0.0135	0.6492
66	0.9787	0.4512	0.7195	0.0006	0.0001	0.3048	0.0000	0.0128	0.6771
67	0.9666	0.4210	0.7401	0.0005	0.0001	0.2788	0.0000	0.0119	0.6970
68	0.9534	0.3939	0.7597	0.0005	0.0001	0.2591	0.0000	0.0112	0.7156
69	0.9329	0.3692	0.7808	0.0005	0.0001	0.2388	0.0000	0.0106	0.7341
70	0.9080	0.3426	0.8000	0.0004	0.0001	0.2113	0.0000	0.0098	0.7583
71	0.9050	0.3217	0.8110	0.0004	0.0001	0.1850	0.0000	0.0095	0.7836
72	0.8934	0.3020	0.8279	0.0004	0.0001	0.1561	0.0000	0.0086	0.8138
73	0.8711	0.2734	0.8788	0.0004	0.0002	0.1318	0.0000	0.0073	0.8512
74	0.8529	0.2297	0.9447	0.0004	0.0002	0.1072	0.0000	0.0063	0.8818
75	0.8622	0.1901	0.9852	0.0003	0.0002	0.0896	0.0000	0.0056	0.8981

76	0.8921	0.1587	0.9868	0.0003	0.0002	0.0800	0.0000	0.0051	0.9112
77	0.8806	0.1350	0.9403	0.0004	0.0003	0.0734	0.0000	0.0045	0.9259
78	0.8903	0.1083	0.8864	0.0004	0.0003	0.0679	0.0000	0.0038	0.9531
79	0.9032	0.0821	0.8384	0.0004	0.0003	0.0589	0.0000	0.0032	0.9827
80	0.9149	0.0614	0.7872	0.0004	0.0003	0.0529	0.0000	0.0026	0.9991
81	0.9409	0.0452	0.7379	0.0005	0.0003	0.0488	0.0000	0.0023	0.9883
82	0.9556	0.0305	0.6758	0.0007	0.0003	0.0478	0.0000	0.0021	0.9863
83	0.9807	0.0230	0.6243	0.0008	0.0003	0.0469	0.0001	0.0018	0.9962
84	0.9866	0.0212	0.5643	0.0009	0.0003	0.0466	0.0001	0.0015	0.9795
85	0.9866	0.0217	0.5053	0.0009	0.0004	0.0462	0.0001	0.0013	0.9807
86	0.9450	0.0226	0.4543	0.0014	0.0005	0.0475	0.0002	0.0012	0.9598
87	0.8924	0.0248	0.4026	0.0022	0.0006	0.0498	0.0004	0.0011	0.9164
88	0.9097	0.0241	0.3464	0.0030	0.0007	0.0518	0.0005	0.0010	0.8811
89	0.9020	0.0236	0.2939	0.0038	0.0008	0.0536	0.0008	0.0009	0.8636
90	0.8670	0.0245	0.2613	0.0056	0.0008	0.0587	0.0014	0.0008	0.8418
91	0.8030	0.0276	0.2490	0.0094	0.0009	0.0658	0.0023	0.0008	0.8000
92	0.7930	0.0305	0.2269	0.0169	0.0013	0.0706	0.0037	0.0009	0.7686
93	0.7893	0.0322	0.2000	0.0290	0.0019	0.0759	0.0061	0.0012	0.7744
94	0.7728	0.0338	0.1655	0.0450	0.0028	0.0839	0.0100	0.0014	0.7859
95	0.7333	0.0376	0.1340	0.0673	0.0040	0.0887	0.0167	0.0015	0.8006
96	0.7003	0.0434	0.0990	0.1024	0.0054	0.0903	0.0261	0.0016	0.8189
97	0.7045	0.0471	0.0719	0.1580	0.0067	0.0923	0.0410	0.0016	0.8157
98	0.7004	0.0521	0.0557	0.2214	0.0077	0.0975	0.0588	0.0018	0.7942
99	0.6973	0.0592	0.0482	0.2813	0.0088	0.1055	0.0782	0.0024	0.7818
100	0.6997	0.0657	0.0370	0.3228	0.0101	0.1165	0.0904	0.0033	0.7824

Table 6. Summary of p-values for flexion-extension, internal-external, and abduction-adduction rotation angles during posteromedial Y-balance task for bilateral control (LR), ACLd, and PFP populations.

Table 7 summarizes the p-values during the posterolateral Y-balance task for all participant groups.

	LR			**ACLd**			**PFP**		
% of Cycle	Flex/Ext	Int/Ext	Ad/Ab	Flex/Ext	Int/Ext	Ad/Ab	Flex/Ext	Int/Ext	Ad/Ab
0	0.8878	0.1059	0.0778	0.4141	0.0174	0.2465	0.0497	0.0064	0.3107
1	0.8478	0.1541	0.0805	0.4108	0.0228	0.2453	0.0406	0.0072	0.3018
2	0.8775	0.1584	0.0904	0.3476	0.0288	0.2200	0.0281	0.0078	0.2947
3	0.9400	0.1563	0.1130	0.2861	0.0333	0.1950	0.0168	0.0088	0.3027
4	0.9929	0.1656	0.1416	0.2332	0.0363	0.1754	0.0092	0.0110	0.3327
5	0.9379	0.1804	0.1914	0.1827	0.0380	0.1503	0.0044	0.0138	0.3866
6	0.8808	0.1990	0.2603	0.1392	0.0370	0.1272	0.0020	0.0152	0.4384
7	0.8429	0.2287	0.3329	0.1066	0.0364	0.1106	0.0009	0.0153	0.4816

8	0.8294	0.2530	0.3939	0.0779	0.0381	0.0925	0.0003	0.0168	0.5428
9	0.8522	0.2580	0.4669	0.0591	0.0393	0.0797	0.0001	0.0181	0.6054
10	0.8431	0.2683	0.5465	0.0446	0.0414	0.0660	0.0001	0.0195	0.6615
11	0.8418	0.2893	0.5802	0.0360	0.0414	0.0545	0.0000	0.0194	0.7149
12	0.8431	0.2903	0.5662	0.0277	0.0421	0.0459	0.0000	0.0193	0.7851
13	0.8357	0.2727	0.5691	0.0230	0.0452	0.0395	0.0000	0.0193	0.8510
14	0.8749	0.2703	0.5436	0.0212	0.0519	0.0321	0.0000	0.0197	0.9310
15	0.8914	0.2813	0.5268	0.0189	0.0576	0.0238	0.0000	0.0199	0.9888
16	0.9194	0.3250	0.5405	0.0168	0.0599	0.0177	0.0000	0.0225	0.9153
17	0.9402	0.3829	0.5522	0.0148	0.0619	0.0135	0.0000	0.0249	0.8623
18	0.9443	0.3961	0.5600	0.0140	0.0611	0.0110	0.0000	0.0273	0.7847
19	0.9838	0.3591	0.5899	0.0138	0.0582	0.0099	0.0000	0.0266	0.7239
20	0.9893	0.3593	0.6454	0.0127	0.0502	0.0095	0.0000	0.0249	0.6928
21	0.9732	0.3727	0.6821	0.0120	0.0408	0.0094	0.0000	0.0239	0.6738
22	0.9704	0.4057	0.7168	0.0111	0.0339	0.0085	0.0000	0.0261	0.6335
23	0.9824	0.4330	0.7556	0.0106	0.0304	0.0079	0.0000	0.0284	0.5752
24	0.9773	0.4439	0.7894	0.0097	0.0284	0.0073	0.0000	0.0307	0.5318
25	0.9980	0.4452	0.8144	0.0099	0.0262	0.0076	0.0000	0.0279	0.5286
26	0.9949	0.4743	0.8273	0.0107	0.0234	0.0087	0.0000	0.0260	0.5371
27	0.9804	0.5043	0.8301	0.0105	0.0206	0.0095	0.0000	0.0225	0.5649
28	0.9488	0.5148	0.8501	0.0095	0.0195	0.0094	0.0000	0.0196	0.5756
29	0.9418	0.4984	0.8882	0.0099	0.0193	0.0092	0.0000	0.0168	0.5807
30	0.9188	0.4364	0.9337	0.0108	0.0183	0.0093	0.0000	0.0152	0.5636
31	0.8953	0.3693	0.9558	0.0113	0.0165	0.0090	0.0000	0.0138	0.5362
32	0.8832	0.3443	0.9618	0.0113	0.0146	0.0085	0.0000	0.0121	0.5077
33	0.8878	0.3414	0.9993	0.0113	0.0130	0.0086	0.0000	0.0100	0.5118
34	0.8892	0.3649	0.9578	0.0118	0.0113	0.0089	0.0000	0.0085	0.5283
35	0.8839	0.3867	0.9379	0.0123	0.0087	0.0099	0.0000	0.0081	0.5431
36	0.8784	0.3916	0.9220	0.0128	0.0066	0.0107	0.0000	0.0080	0.5559
37	0.8875	0.3902	0.9026	0.0128	0.0052	0.0109	0.0000	0.0084	0.5516
38	0.8800	0.4066	0.8782	0.0124	0.0047	0.0106	0.0000	0.0088	0.5373
39	0.8922	0.4243	0.8510	0.0122	0.0040	0.0104	0.0000	0.0087	0.5389
40	0.9032	0.4358	0.8426	0.0123	0.0036	0.0103	0.0000	0.0086	0.5502
41	0.9334	0.4445	0.8349	0.0123	0.0033	0.0096	0.0000	0.0080	0.5585
42	0.9477	0.4394	0.8332	0.0122	0.0030	0.0092	0.0000	0.0076	0.5774
43	0.9655	0.4225	0.8243	0.0119	0.0025	0.0094	0.0000	0.0075	0.6033
44	0.9808	0.4003	0.8042	0.0118	0.0021	0.0101	0.0000	0.0078	0.6287
45	0.9958	0.3947	0.7952	0.0118	0.0017	0.0110	0.0001	0.0083	0.6456
46	0.9758	0.3967	0.8023	0.0117	0.0016	0.0115	0.0001	0.0087	0.6456
47	0.9644	0.3912	0.8061	0.0112	0.0015	0.0116	0.0001	0.0088	0.6443
48	0.9614	0.3817	0.7943	0.0107	0.0015	0.0117	0.0001	0.0087	0.6487
49	0.9653	0.3749	0.7800	0.0101	0.0015	0.0126	0.0001	0.0084	0.6519
50	0.9597	0.3807	0.7711	0.0095	0.0014	0.0135	0.0001	0.0083	0.6612

51	0.9586	0.3933	0.7508	0.0092	0.0013	0.0150	0.0001	0.0080	0.6787
52	0.9631	0.3995	0.7305	0.0086	0.0014	0.0158	0.0001	0.0076	0.7010
53	0.9622	0.4050	0.7207	0.0080	0.0014	0.0162	0.0001	0.0068	0.7210
54	0.9522	0.4069	0.7313	0.0073	0.0014	0.0160	0.0001	0.0059	0.7370
55	0.9421	0.4253	0.7367	0.0067	0.0014	0.0154	0.0001	0.0049	0.7438
56	0.9334	0.4446	0.7283	0.0061	0.0015	0.0148	0.0001	0.0043	0.7482
57	0.9309	0.4622	0.7325	0.0055	0.0016	0.0139	0.0001	0.0040	0.7416
58	0.9239	0.4670	0.7383	0.0049	0.0016	0.0127	0.0001	0.0038	0.7422
59	0.9184	0.4777	0.7467	0.0044	0.0017	0.0119	0.0001	0.0036	0.7483
60	0.9067	0.4951	0.7567	0.0038	0.0017	0.0107	0.0001	0.0034	0.7571
61	0.8990	0.5192	0.7690	0.0034	0.0019	0.0096	0.0001	0.0033	0.7586
62	0.9001	0.5395	0.7800	0.0030	0.0020	0.0086	0.0001	0.0033	0.7638
63	0.8919	0.5561	0.7887	0.0026	0.0020	0.0078	0.0002	0.0032	0.7769
64	0.8925	0.5519	0.7963	0.0023	0.0020	0.0069	0.0002	0.0031	0.7960
65	0.8916	0.5578	0.8021	0.0021	0.0021	0.0063	0.0001	0.0030	0.7996
66	0.8864	0.5706	0.8204	0.0021	0.0023	0.0058	0.0001	0.0031	0.7988
67	0.8792	0.5704	0.8399	0.0020	0.0024	0.0053	0.0001	0.0033	0.7896
68	0.8608	0.5590	0.8512	0.0017	0.0024	0.0047	0.0001	0.0034	0.7793
69	0.8795	0.5371	0.8712	0.0016	0.0022	0.0042	0.0001	0.0035	0.7629
70	0.8986	0.5264	0.8955	0.0014	0.0021	0.0039	0.0001	0.0040	0.7594
71	0.8913	0.5169	0.9264	0.0014	0.0019	0.0040	0.0000	0.0045	0.7636
72	0.8711	0.4820	0.9630	0.0014	0.0019	0.0043	0.0000	0.0051	0.7680
73	0.8793	0.4615	0.9849	0.0014	0.0020	0.0049	0.0000	0.0060	0.7640
74	0.8728	0.4457	0.9430	0.0014	0.0024	0.0053	0.0000	0.0072	0.7690
75	0.8677	0.4216	0.9318	0.0014	0.0027	0.0059	0.0000	0.0088	0.7788
76	0.8620	0.3694	0.9198	0.0014	0.0028	0.0065	0.0000	0.0101	0.7936
77	0.8814	0.3211	0.8897	0.0014	0.0029	0.0073	0.0000	0.0109	0.7980
78	0.8818	0.3001	0.8566	0.0015	0.0031	0.0077	0.0000	0.0117	0.7969
79	0.8889	0.2951	0.8227	0.0015	0.0035	0.0079	0.0000	0.0120	0.8034
80	0.8927	0.2888	0.7879	0.0016	0.0040	0.0079	0.0000	0.0131	0.8190
81	0.8891	0.2795	0.7514	0.0019	0.0045	0.0084	0.0000	0.0137	0.8556
82	0.8620	0.2661	0.7090	0.0022	0.0044	0.0100	0.0000	0.0134	0.8959
83	0.8345	0.2648	0.6628	0.0024	0.0046	0.0117	0.0000	0.0127	0.9415
84	0.8414	0.2584	0.6098	0.0026	0.0051	0.0141	0.0000	0.0121	0.9777
85	0.8385	0.2492	0.5615	0.0033	0.0061	0.0171	0.0000	0.0129	0.9683
86	0.8179	0.2270	0.5103	0.0040	0.0069	0.0209	0.0000	0.0141	0.9564
87	0.7880	0.1972	0.4567	0.0049	0.0076	0.0248	0.0000	0.0151	0.9366
88	0.7456	0.1755	0.4178	0.0058	0.0082	0.0305	0.0000	0.0162	0.8980
89	0.7573	0.1570	0.3473	0.0073	0.0094	0.0357	0.0000	0.0172	0.8608
90	0.7461	0.1418	0.2979	0.0113	0.0104	0.0442	0.0000	0.0173	0.8249
91	0.7820	0.1307	0.2772	0.0179	0.0115	0.0509	0.0001	0.0163	0.7920
92	0.7917	0.1343	0.2739	0.0260	0.0117	0.0558	0.0002	0.0144	0.7635
93	0.8037	0.1478	0.2554	0.0367	0.0116	0.0607	0.0003	0.0121	0.7276

94	0.8393	0.1707	0.2243	0.0544	0.0107	0.0653	0.0009	0.0099	0.6821
95	0.8970	0.1897	0.1837	0.0868	0.0101	0.0740	0.0028	0.0085	0.6200
96	0.9479	0.1884	0.1487	0.1322	0.0101	0.0809	0.0065	0.0076	0.5673
97	0.9728	0.1707	0.1336	0.1879	0.0092	0.0851	0.0114	0.0063	0.5415
98	0.9277	0.1667	0.1273	0.2604	0.0079	0.0868	0.0200	0.0050	0.5258
99	0.9061	0.1760	0.1046	0.3434	0.0073	0.0840	0.0345	0.0043	0.5342
100	0.8714	0.1616	0.0811	0.4303	0.0063	0.0855	0.0553	0.0034	0.5401

Table 7. Summary of p-values for flexion-extension, internal-external, and abduction-adduction rotation angles during posterolateral Y-balance task for bilateral control (LR), ACLd, and PFP populations.

Bilateral Differences in Control Data

During the posteromedial Y-balance task significant differences ($p<0.05$) were observed for internal-external rotation between 81-97% and for abduction-adduction between 0-3% and at 99% of the cycle. There were no significant differences observed during the posterolateral Y-balance task. One control participant data set had to be excluded for reasons mentioned in Section 4.1.

ACLd Group Posteromedial

Data from the posteromedial Y-balance shows an increase in external rotation for 100% of the cycle, an increase in abduction rotation for 82-88% of the cycle, and an increase in flexion for 9-94% of the cycle for ACLd participants compared to controls. Two ACLd participant data sets were excluded for reasons mentioned in Section 4.1.

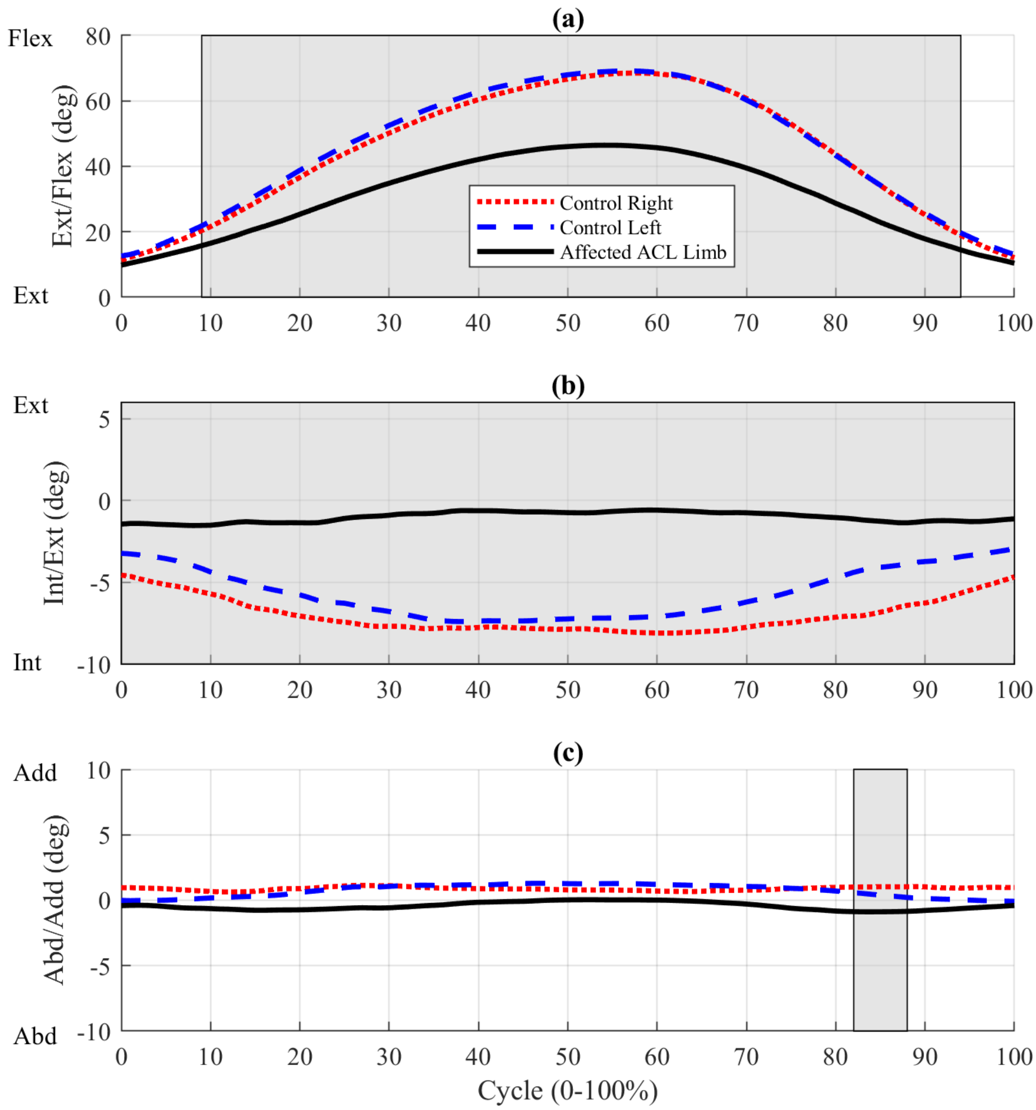

Figure 9. Rotation angles during posteromedial Y-balance for ACLd group. (a) Flexion-extension. Significantly lower ACLd flexion rotation between 9-94% (b) Internal-external. Significantly less ACLd internal rotation for 100% of the cycle. (c) Abduction-adduction. Significantly less ACLd adduction rotation between 82-88%. Shaded regions indicate areas of significant differences.

ACLd Group Posterolateral

Data from the posterolateral Y-balance shows an increase in external rotation for 93% of the cycle, an increase in abduction rotation between 12-90% of the cycle, and an increase in flexion from 10-93% of the cycle for ACLd participants compared to controls. Two ACL participant data sets were excluded for reasons mentioned in Section 4.1.

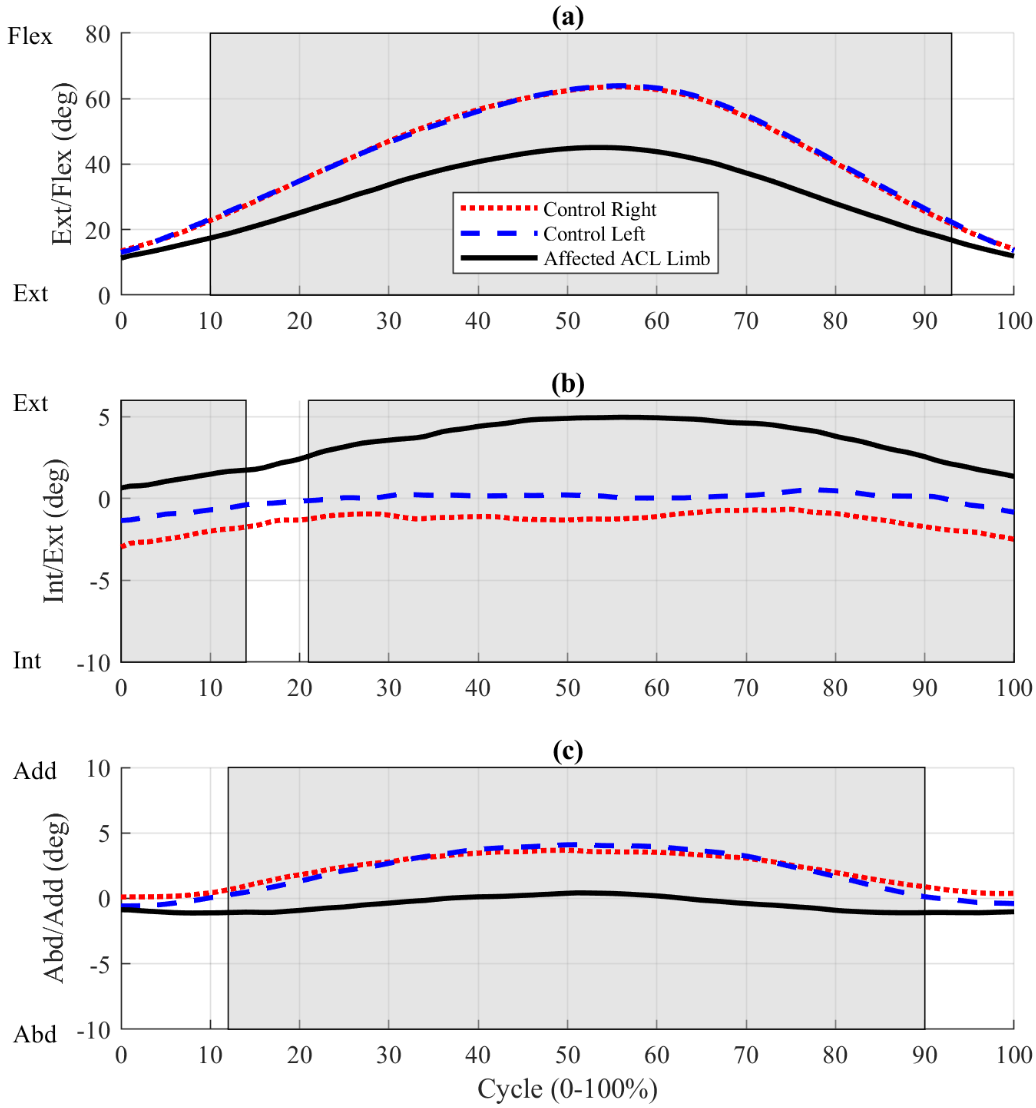

Figure 10. Rotation angles during posterolateral Y-balance for ACLd group. (a) Flexion-extension. Significantly lower ACLd flexion rotation between 10-93% (b) Internal-external. Significantly more ACLd external rotation between 0-13% and 21-100% of the cycle. (c) Abduction-adduction. Significantly less ACLd adduction rotation between 12-90%. Shaded regions indicate areas of significant differences.

PFP Group Posteromedial

Data from the posteromedial Y-balance shows an increase in external rotation for 100% of the cycle and an increase in flexion for 4-97% of the cycle for PFP participants compared to controls. There were no significant differences in abduction-adduction rotation angles. Two ACL participant data sets had to be excluded due to unclear cycle definitions. One PFP participant data set was excluded for reasons mentioned in Section 4.1.

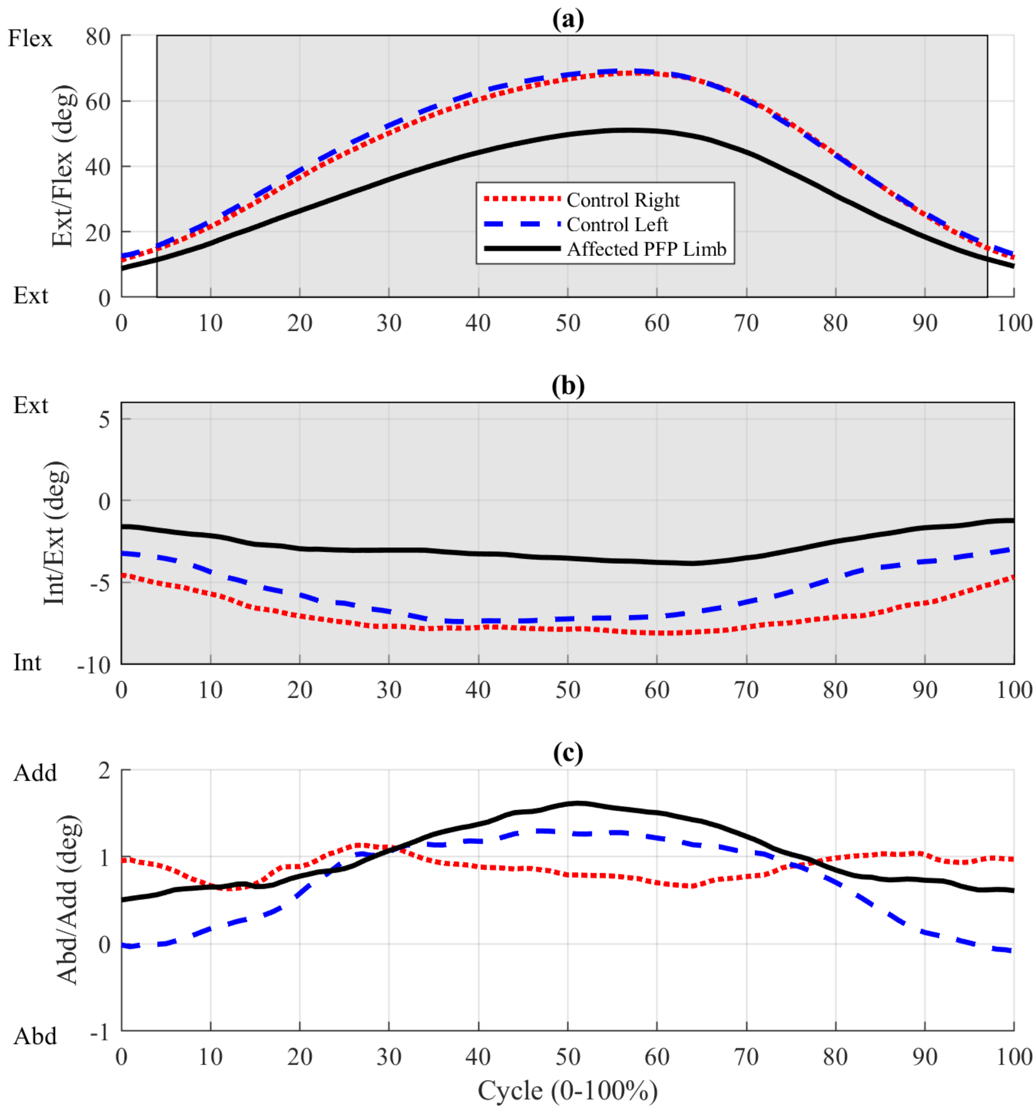

Figure 11. Rotation angles during posteromedial Y-balance for PFP group. (a) Flexion-extension. Significantly lower PFP flexion rotation between 4-97% (b) Internal-external. Significantly less PFP internal rotation for 100% of the cycle. (c) Abduction-adduction. Shaded regions indicate areas of significant differences.

PFP Group Posterolateral

Data from the posterolateral Y-balance shows an increase in external rotation for 100% of the cycle and an increase in flexion from 0-99% of the cycle for PFP participants compared to controls. There were no significant differences in abduction-adduction rotation angles. One PFP participant data set was excluded for reasons mentioned in Section 4.1.

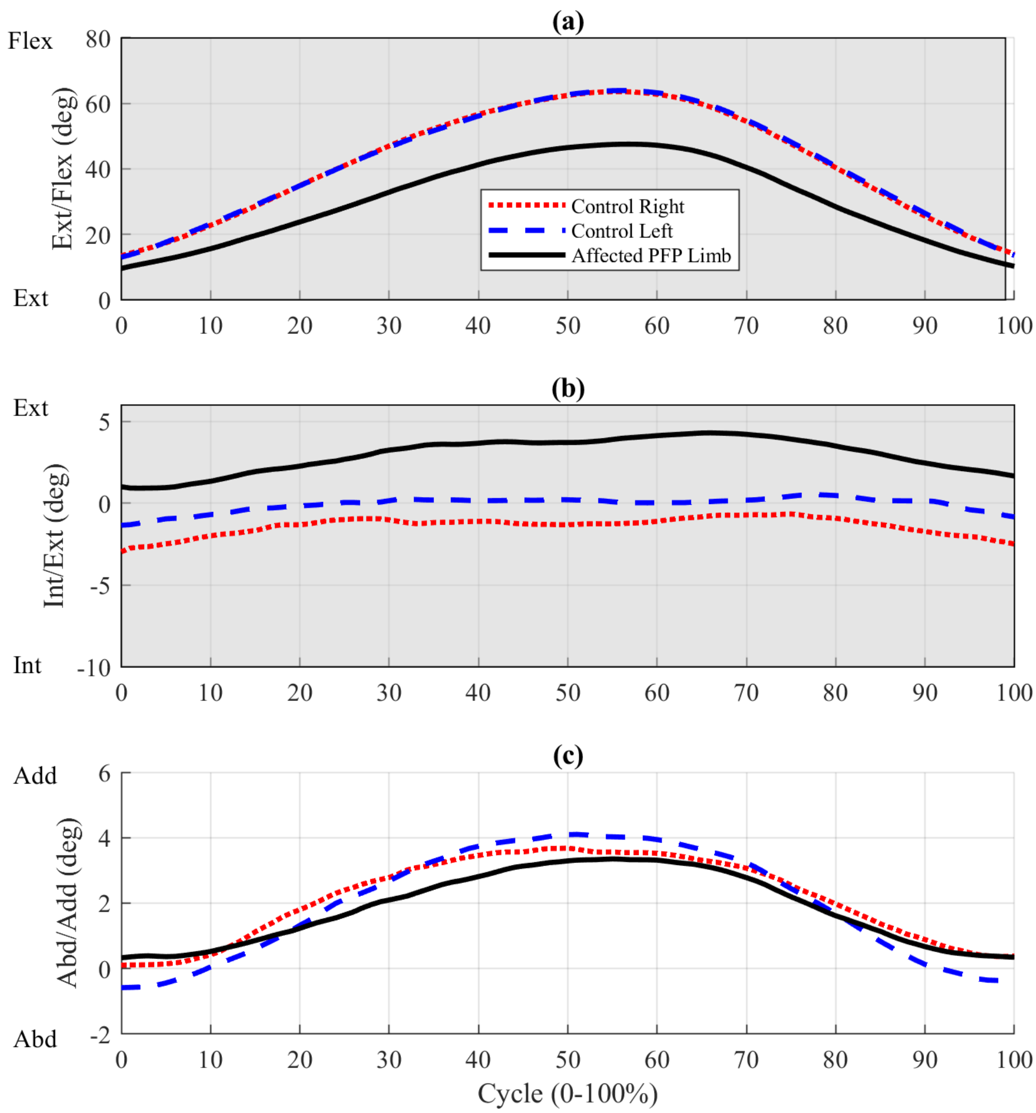

Figure 12. Rotation angles during posterolateral Y-balance for PFP group. (a) Flexion-extension. Significantly lower PFP flexion rotation between 0-99%% of the cycle. (b) Internal-external. Significantly more PFP external rotation for 100% of the cycle. (c) Abduction-adduction. Shaded regions indicate areas of significant differences.

4.1.5 Medial and lateral single leg squats

Table 8 summarizes the p-values during the medial SLS task for all participant groups.

	LR			ACLd			PFP		
% of Cycle	Flex/Ext	Int/Ext	Ad/Ab	Flex/Ext	Int/Ext	Ad/Ab	Flex/Ext	Int/Ext	Ad/Ab
0	0.6231	0.5194	0.7170	0.0424	0.0004	0.0963	0.0064	0.0605	0.7339
1	0.6529	0.4747	0.6780	0.0398	0.0003	0.1145	0.0048	0.0505	0.7306
2	0.6755	0.4472	0.6811	0.0280	0.0003	0.1411	0.0028	0.0427	0.7088
3	0.6953	0.4253	0.6917	0.0218	0.0003	0.1608	0.0019	0.0344	0.6886
4	0.7075	0.3997	0.6978	0.0156	0.0003	0.1779	0.0013	0.0283	0.6485
5	0.6885	0.3708	0.7011	0.0111	0.0003	0.1979	0.0009	0.0252	0.6142
6	0.6786	0.3476	0.7087	0.0083	0.0003	0.2183	0.0006	0.0247	0.6070
7	0.7098	0.3302	0.7283	0.0069	0.0004	0.2367	0.0006	0.0260	0.6145
8	0.7399	0.3147	0.7309	0.0054	0.0004	0.2592	0.0006	0.0271	0.6303
9	0.7482	0.3037	0.7291	0.0042	0.0005	0.2791	0.0006	0.0282	0.6412
10	0.7178	0.3048	0.7198	0.0034	0.0005	0.2842	0.0006	0.0310	0.6821
11	0.6841	0.3105	0.6991	0.0027	0.0006	0.2807	0.0006	0.0349	0.7555
12	0.7073	0.3166	0.6801	0.0021	0.0005	0.2788	0.0006	0.0365	0.8214
13	0.7498	0.3267	0.6658	0.0018	0.0005	0.2820	0.0006	0.0365	0.8606
14	0.7613	0.3362	0.6673	0.0015	0.0005	0.2895	0.0006	0.0366	0.8837
15	0.7818	0.3524	0.6764	0.0012	0.0004	0.2945	0.0006	0.0401	0.9371
16	0.7884	0.3534	0.6926	0.0010	0.0004	0.2971	0.0006	0.0438	0.9871
17	0.8114	0.3517	0.7012	0.0008	0.0004	0.3047	0.0006	0.0459	0.9892
18	0.8479	0.3579	0.6926	0.0007	0.0004	0.3151	0.0006	0.0492	0.9734
19	0.8717	0.3667	0.6719	0.0006	0.0004	0.3161	0.0005	0.0507	0.9447
20	0.8983	0.3648	0.6774	0.0005	0.0004	0.3158	0.0005	0.0534	0.9111
21	0.8829	0.3633	0.6893	0.0004	0.0004	0.3178	0.0004	0.0547	0.8834
22	0.8789	0.3707	0.6692	0.0003	0.0004	0.3238	0.0004	0.0547	0.8639
23	0.8939	0.3740	0.6495	0.0003	0.0004	0.3273	0.0004	0.0525	0.8402
24	0.9092	0.3775	0.6488	0.0003	0.0004	0.3318	0.0003	0.0491	0.8267
25	0.9029	0.3898	0.6523	0.0003	0.0003	0.3295	0.0003	0.0462	0.8424
26	0.8851	0.4030	0.6811	0.0002	0.0003	0.3351	0.0003	0.0449	0.8699
27	0.8926	0.3968	0.7281	0.0002	0.0003	0.3624	0.0003	0.0461	0.8864
28	0.8779	0.3964	0.7680	0.0002	0.0003	0.3873	0.0003	0.0458	0.8846
29	0.8746	0.4028	0.8076	0.0002	0.0002	0.3980	0.0003	0.0432	0.8884
30	0.8645	0.4198	0.8617	0.0003	0.0002	0.4234	0.0003	0.0395	0.9097
31	0.8496	0.4467	0.9205	0.0003	0.0001	0.4566	0.0002	0.0379	0.9276
32	0.8316	0.4701	0.9611	0.0004	0.0001	0.4898	0.0003	0.0368	0.9474
33	0.8134	0.4836	0.9835	0.0004	0.0001	0.5115	0.0003	0.0353	0.9708
34	0.8016	0.4817	0.9962	0.0005	0.0001	0.5199	0.0003	0.0369	0.9891

35	0.7906	0.4781	0.9761	0.0006	0.0001	0.5272	0.0003	0.0388	0.9910
36	0.7834	0.4870	0.9539	0.0007	0.0001	0.5404	0.0003	0.0400	0.9593
37	0.7604	0.4960	0.9462	0.0008	0.0001	0.5648	0.0003	0.0399	0.9289
38	0.7418	0.4946	0.9585	0.0009	0.0001	0.5793	0.0003	0.0401	0.8990
39	0.7236	0.4828	0.9760	0.0010	0.0001	0.5902	0.0003	0.0418	0.8816
40	0.7113	0.4702	0.9768	0.0011	0.0001	0.6102	0.0004	0.0425	0.8699
41	0.6994	0.4672	0.9691	0.0012	0.0001	0.6364	0.0004	0.0411	0.8585
42	0.6921	0.4677	0.9608	0.0013	0.0001	0.6707	0.0004	0.0420	0.8470
43	0.6817	0.4565	0.9531	0.0014	0.0001	0.6896	0.0005	0.0438	0.8415
44	0.6702	0.4474	0.9500	0.0015	0.0001	0.7026	0.0005	0.0460	0.8265
45	0.6640	0.4476	0.9330	0.0016	0.0001	0.7219	0.0005	0.0475	0.8041
46	0.6616	0.4571	0.9111	0.0016	0.0000	0.7498	0.0005	0.0497	0.7845
47	0.6556	0.4694	0.8943	0.0017	0.0000	0.7618	0.0006	0.0515	0.7669
48	0.6540	0.4839	0.8725	0.0017	0.0000	0.7624	0.0006	0.0536	0.7589
49	0.6571	0.4989	0.8510	0.0018	0.0000	0.7570	0.0007	0.0555	0.7494
50	0.6594	0.5071	0.8408	0.0018	0.0000	0.7488	0.0007	0.0578	0.7483
51	0.6547	0.5085	0.8393	0.0018	0.0000	0.7403	0.0008	0.0597	0.7519
52	0.6535	0.5192	0.8395	0.0019	0.0000	0.7427	0.0008	0.0616	0.7499
53	0.6534	0.5302	0.8272	0.0019	0.0000	0.7531	0.0008	0.0628	0.7454
54	0.6481	0.5331	0.8101	0.0019	0.0000	0.7618	0.0009	0.0636	0.7444
55	0.6403	0.5157	0.8030	0.0018	0.0000	0.7650	0.0009	0.0642	0.7361
56	0.6371	0.5083	0.8003	0.0018	0.0000	0.7685	0.0009	0.0651	0.7308
57	0.6363	0.5017	0.8031	0.0018	0.0000	0.7750	0.0009	0.0670	0.7318
58	0.6314	0.4966	0.8005	0.0017	0.0000	0.7749	0.0009	0.0692	0.7321
59	0.6264	0.4886	0.7973	0.0015	0.0000	0.7768	0.0008	0.0693	0.7364
60	0.6221	0.4793	0.8008	0.0013	0.0000	0.7819	0.0008	0.0676	0.7431
61	0.6207	0.4750	0.7974	0.0011	0.0000	0.7727	0.0008	0.0649	0.7440
62	0.6230	0.4741	0.7887	0.0010	0.0000	0.7560	0.0007	0.0615	0.7366
63	0.6246	0.4782	0.7907	0.0008	0.0000	0.7363	0.0007	0.0591	0.7292
64	0.6320	0.4815	0.7881	0.0006	0.0000	0.7170	0.0006	0.0570	0.7261
65	0.6323	0.4840	0.7751	0.0005	0.0001	0.6949	0.0006	0.0541	0.7370
66	0.6304	0.4944	0.7690	0.0003	0.0001	0.6680	0.0005	0.0527	0.7550
67	0.6293	0.5124	0.7638	0.0002	0.0001	0.6437	0.0005	0.0509	0.7672
68	0.6192	0.5317	0.7567	0.0002	0.0001	0.6205	0.0005	0.0491	0.7853
69	0.6038	0.5429	0.7396	0.0001	0.0001	0.6007	0.0004	0.0476	0.8106
70	0.5915	0.5426	0.7235	0.0001	0.0001	0.5865	0.0004	0.0464	0.8291
71	0.5879	0.5264	0.7209	0.0001	0.0001	0.5746	0.0004	0.0457	0.8500
72	0.5753	0.4961	0.7376	0.0000	0.0001	0.5623	0.0004	0.0437	0.8700
73	0.5487	0.4649	0.7524	0.0000	0.0001	0.5481	0.0004	0.0431	0.8904
74	0.5260	0.4403	0.7802	0.0000	0.0001	0.5349	0.0004	0.0445	0.9123
75	0.5071	0.4269	0.8171	0.0000	0.0001	0.5269	0.0003	0.0479	0.9269
76	0.4947	0.4113	0.8575	0.0000	0.0001	0.5200	0.0003	0.0521	0.9494
77	0.4975	0.3914	0.8952	0.0000	0.0001	0.5116	0.0003	0.0576	0.9671

78	0.4971	0.3608	0.9206	0.0000	0.0001	0.5045	0.0004	0.0664	0.9734
79	0.4738	0.3360	0.9466	0.0000	0.0001	0.4979	0.0004	0.0770	0.9799
80	0.4543	0.3142	0.9690	0.0000	0.0001	0.4858	0.0004	0.0871	0.9937
81	0.4711	0.2930	0.9896	0.0000	0.0002	0.4765	0.0004	0.0934	0.9939
82	0.4888	0.2762	0.9991	0.0000	0.0002	0.4611	0.0004	0.1007	0.9929
83	0.4883	0.2724	0.9973	0.0000	0.0003	0.4501	0.0005	0.1110	0.9854
84	0.5001	0.2704	0.9925	0.0000	0.0003	0.4233	0.0007	0.1200	0.9745
85	0.5354	0.2708	0.9707	0.0000	0.0003	0.3989	0.0007	0.1197	0.9877
86	0.5713	0.2783	0.9483	0.0001	0.0004	0.3981	0.0009	0.1256	0.9747
87	0.5865	0.2894	0.9072	0.0001	0.0004	0.4022	0.0010	0.1357	0.9533
88	0.6200	0.2856	0.8559	0.0002	0.0004	0.3907	0.0012	0.1448	0.9405
89	0.6118	0.2805	0.8023	0.0003	0.0005	0.3731	0.0014	0.1485	0.9107
90	0.5964	0.2845	0.7714	0.0006	0.0005	0.3610	0.0018	0.1490	0.8801
91	0.6261	0.2971	0.7476	0.0011	0.0004	0.3424	0.0020	0.1450	0.8624
92	0.6505	0.3118	0.7022	0.0019	0.0005	0.3202	0.0018	0.1373	0.8634
93	0.6632	0.3253	0.6456	0.0031	0.0005	0.2859	0.0021	0.1322	0.8695
94	0.6322	0.3274	0.5846	0.0049	0.0006	0.2498	0.0025	0.1242	0.8779
95	0.6181	0.3194	0.5403	0.0070	0.0006	0.2126	0.0025	0.1098	0.8950
96	0.6104	0.3127	0.5087	0.0102	0.0006	0.1828	0.0023	0.0966	0.9031
97	0.6207	0.3174	0.4954	0.0147	0.0006	0.1580	0.0026	0.0872	0.9069
98	0.6278	0.3384	0.4727	0.0209	0.0006	0.1344	0.0031	0.0790	0.9006
99	0.6537	0.3649	0.4405	0.0287	0.0006	0.1124	0.0033	0.0703	0.9077
100	0.6427	0.3853	0.4243	0.0371	0.0006	0.0925	0.0042	0.0657	0.9173

Table 8. Summary of p-values for flexion-extension, internal-external, and abduction-adduction rotation angles during medial SLS task for bilateral control (LR), ACLd, and PFP populations.

Table 9 summarizes the p-values during the lateral SLS task for all participant groups.

	LR			**ACLd**			**PFP**		
% of Cycle	Flex/Ext	Int/Ext	Ad/Ab	Flex/Ext	Int/Ext	Ad/Ab	Flex/Ext	Int/Ext	Ad/Ab
0	0.6369	0.9740	0.2530	0.3906	0.1185	0.7175	0.0319	0.3950	0.5004
1	0.5996	0.9572	0.2797	0.2865	0.1304	0.6017	0.0216	0.4663	0.5799
2	0.6024	0.9655	0.3215	0.2399	0.1242	0.5329	0.0153	0.4840	0.6321
3	0.6246	0.9864	0.3831	0.2006	0.1139	0.4949	0.0111	0.4946	0.6786
4	0.6382	0.9994	0.4551	0.1653	0.1055	0.4690	0.0074	0.5060	0.7244
5	0.6568	0.9932	0.5044	0.1253	0.0978	0.4463	0.0047	0.5112	0.7887
6	0.6747	0.9978	0.5517	0.0944	0.0885	0.4322	0.0032	0.5027	0.8633
7	0.6963	0.9971	0.5979	0.0717	0.0837	0.4117	0.0023	0.4937	0.9294
8	0.7156	0.9837	0.6363	0.0511	0.0803	0.3845	0.0017	0.4734	0.9932
9	0.7446	0.9375	0.6855	0.0349	0.0764	0.3662	0.0012	0.4481	0.9622
10	0.8001	0.8786	0.7431	0.0234	0.0730	0.3524	0.0009	0.4277	0.9273
11	0.8084	0.8193	0.8297	0.0187	0.0720	0.3436	0.0007	0.4143	0.8911

12	0.8280	0.7897	0.8913	0.0147	0.0718	0.3312	0.0005	0.4261	0.8419
13	0.8384	0.7957	0.9254	0.0116	0.0682	0.3182	0.0005	0.4443	0.7757
14	0.8507	0.7983	0.9386	0.0083	0.0610	0.3169	0.0005	0.4424	0.7099
15	0.8493	0.8000	0.9403	0.0060	0.0558	0.3209	0.0004	0.4329	0.6707
16	0.8547	0.8296	0.9469	0.0046	0.0526	0.3317	0.0003	0.4320	0.6504
17	0.8748	0.8727	0.9600	0.0040	0.0495	0.3487	0.0003	0.4319	0.6379
18	0.9213	0.9036	0.9407	0.0036	0.0440	0.3659	0.0004	0.4259	0.6266
19	0.9290	0.9080	0.8931	0.0034	0.0403	0.3811	0.0004	0.4307	0.5966
20	0.9189	0.9232	0.8599	0.0034	0.0367	0.3925	0.0004	0.4289	0.5668
21	0.8782	0.9552	0.8562	0.0035	0.0330	0.4080	0.0004	0.4188	0.5643
22	0.8510	0.9704	0.8434	0.0036	0.0294	0.4223	0.0005	0.4026	0.5683
23	0.8495	0.9608	0.8292	0.0036	0.0257	0.4396	0.0005	0.3769	0.5573
24	0.8516	0.9520	0.8300	0.0037	0.0229	0.4411	0.0005	0.3495	0.5421
25	0.8542	0.9288	0.8458	0.0038	0.0223	0.4426	0.0006	0.3333	0.5450
26	0.8212	0.8870	0.8671	0.0040	0.0235	0.4465	0.0007	0.3249	0.5471
27	0.7842	0.8603	0.8977	0.0044	0.0250	0.4606	0.0007	0.3144	0.5447
28	0.7652	0.8590	0.9294	0.0047	0.0255	0.4746	0.0008	0.3164	0.5415
29	0.7655	0.8788	0.9666	0.0052	0.0225	0.4856	0.0008	0.3171	0.5365
30	0.7646	0.8910	0.9928	0.0058	0.0193	0.4971	0.0009	0.3231	0.5341
31	0.7571	0.8832	0.9520	0.0066	0.0167	0.5195	0.0009	0.3279	0.5398
32	0.7376	0.8712	0.9252	0.0073	0.0149	0.5368	0.0010	0.3317	0.5373
33	0.7137	0.8713	0.9224	0.0082	0.0129	0.5405	0.0012	0.3413	0.5209
34	0.6854	0.8647	0.9395	0.0098	0.0119	0.5297	0.0014	0.3522	0.4963
35	0.6663	0.8646	0.9423	0.0117	0.0116	0.5191	0.0014	0.3556	0.4788
36	0.6604	0.8667	0.9285	0.0130	0.0113	0.5149	0.0016	0.3520	0.4667
37	0.6488	0.8688	0.9216	0.0139	0.0106	0.5189	0.0019	0.3476	0.4678
38	0.6438	0.8778	0.9161	0.0148	0.0097	0.5191	0.0022	0.3463	0.4744
39	0.6335	0.8808	0.9067	0.0163	0.0090	0.5143	0.0023	0.3388	0.4716
40	0.6242	0.8751	0.9054	0.0179	0.0081	0.5157	0.0024	0.3229	0.4611
41	0.6100	0.8728	0.9131	0.0197	0.0071	0.5231	0.0027	0.3133	0.4552
42	0.6094	0.8709	0.9140	0.0213	0.0066	0.5280	0.0030	0.3076	0.4519
43	0.6064	0.8716	0.9063	0.0228	0.0065	0.5284	0.0032	0.3055	0.4492
44	0.6021	0.8777	0.8876	0.0244	0.0065	0.5235	0.0033	0.3054	0.4347
45	0.5902	0.8855	0.8737	0.0252	0.0063	0.5219	0.0033	0.3011	0.4267
46	0.5855	0.8919	0.8722	0.0263	0.0060	0.5179	0.0033	0.2949	0.4242
47	0.5830	0.8942	0.8796	0.0274	0.0056	0.5192	0.0035	0.2874	0.4235
48	0.5802	0.8980	0.8920	0.0280	0.0055	0.5216	0.0038	0.2853	0.4215
49	0.5737	0.9014	0.8932	0.0285	0.0055	0.5201	0.0039	0.2818	0.4195
50	0.5686	0.9066	0.8906	0.0282	0.0054	0.5184	0.0040	0.2803	0.4199
51	0.5652	0.9113	0.8865	0.0275	0.0052	0.5070	0.0041	0.2763	0.4147
52	0.5653	0.9058	0.8866	0.0274	0.0051	0.4994	0.0042	0.2705	0.4062
53	0.5674	0.9086	0.8878	0.0264	0.0050	0.4931	0.0043	0.2670	0.3956
54	0.5670	0.9198	0.8880	0.0248	0.0050	0.4845	0.0044	0.2670	0.3920

55	0.5642	0.9273	0.8847	0.0232	0.0050	0.4791	0.0043	0.2677	0.3905
56	0.5701	0.9189	0.8829	0.0215	0.0048	0.4784	0.0041	0.2670	0.3864
57	0.5748	0.9107	0.8855	0.0198	0.0046	0.4779	0.0039	0.2649	0.3869
58	0.5776	0.9088	0.8862	0.0178	0.0044	0.4762	0.0037	0.2609	0.3976
59	0.5805	0.9071	0.8792	0.0158	0.0043	0.4692	0.0036	0.2596	0.4071
60	0.5900	0.9051	0.8740	0.0140	0.0044	0.4712	0.0033	0.2619	0.4172
61	0.5912	0.8960	0.8589	0.0123	0.0045	0.4748	0.0031	0.2642	0.4242
62	0.5898	0.8903	0.8436	0.0107	0.0044	0.4676	0.0028	0.2613	0.4180
63	0.5836	0.8864	0.8323	0.0090	0.0043	0.4580	0.0026	0.2524	0.4073
64	0.5902	0.8827	0.8279	0.0075	0.0042	0.4537	0.0024	0.2406	0.3960
65	0.5957	0.8772	0.8378	0.0064	0.0041	0.4514	0.0023	0.2316	0.3854
66	0.6084	0.8777	0.8582	0.0054	0.0040	0.4478	0.0020	0.2268	0.3755
67	0.6145	0.8841	0.8661	0.0046	0.0039	0.4427	0.0019	0.2248	0.3669
68	0.6222	0.8820	0.8657	0.0038	0.0041	0.4345	0.0018	0.2299	0.3563
69	0.6117	0.8729	0.8684	0.0032	0.0043	0.4230	0.0016	0.2399	0.3544
70	0.6005	0.8583	0.8723	0.0028	0.0050	0.4123	0.0014	0.2521	0.3564
71	0.6060	0.8340	0.8709	0.0024	0.0059	0.4026	0.0013	0.2659	0.3477
72	0.6077	0.8226	0.8732	0.0020	0.0071	0.3901	0.0014	0.2825	0.3337
73	0.6069	0.8254	0.8712	0.0018	0.0079	0.3819	0.0013	0.3011	0.3201
74	0.5885	0.8331	0.8678	0.0017	0.0082	0.3786	0.0014	0.3143	0.3089
75	0.5960	0.8198	0.8705	0.0017	0.0085	0.3715	0.0014	0.3282	0.2990
76	0.5896	0.7986	0.8784	0.0017	0.0090	0.3655	0.0013	0.3473	0.2930
77	0.5881	0.7659	0.8804	0.0016	0.0102	0.3609	0.0011	0.3655	0.2875
78	0.5722	0.7484	0.8853	0.0016	0.0120	0.3579	0.0012	0.3849	0.2838
79	0.5520	0.7406	0.8829	0.0017	0.0143	0.3439	0.0012	0.4066	0.2846
80	0.5438	0.7333	0.8728	0.0019	0.0172	0.3298	0.0013	0.4348	0.2880
81	0.5322	0.7145	0.8632	0.0020	0.0204	0.3169	0.0013	0.4567	0.2868
82	0.5228	0.7000	0.8581	0.0019	0.0252	0.3116	0.0012	0.4813	0.2923
83	0.5177	0.6951	0.8672	0.0022	0.0320	0.3096	0.0012	0.5060	0.3003
84	0.5191	0.6769	0.8910	0.0026	0.0391	0.3120	0.0013	0.5266	0.3092
85	0.5113	0.6481	0.9073	0.0031	0.0455	0.3108	0.0012	0.5380	0.3235
86	0.5081	0.6140	0.9205	0.0038	0.0516	0.3081	0.0012	0.5412	0.3295
87	0.5209	0.5953	0.9397	0.0043	0.0579	0.2914	0.0012	0.5399	0.3322
88	0.5340	0.5762	0.9648	0.0052	0.0617	0.2808	0.0014	0.5194	0.3425
89	0.5557	0.5664	0.9863	0.0068	0.0640	0.2770	0.0015	0.5064	0.3685
90	0.5662	0.5777	0.9718	0.0091	0.0651	0.2856	0.0012	0.4990	0.3964
91	0.5807	0.5916	0.9053	0.0135	0.0669	0.3030	0.0014	0.4933	0.4426
92	0.5831	0.6008	0.8140	0.0191	0.0699	0.3071	0.0019	0.4772	0.4857
93	0.5950	0.6111	0.7258	0.0281	0.0721	0.3070	0.0028	0.4721	0.5211
94	0.6014	0.6390	0.6518	0.0409	0.0728	0.3033	0.0039	0.4752	0.5536
95	0.5953	0.6790	0.5965	0.0586	0.0771	0.3107	0.0048	0.4893	0.5890
96	0.6138	0.7152	0.5350	0.0868	0.0833	0.3214	0.0063	0.5099	0.6401
97	0.6272	0.7298	0.4621	0.1273	0.0897	0.3375	0.0083	0.5221	0.7088

98	0.6439	0.7322	0.3935	0.1842	0.0968	0.3530	0.0124	0.5286	0.8095
99	0.6151	0.7359	0.3483	0.2479	0.1076	0.3654	0.0170	0.5397	0.9084
100	0.6107	0.7430	0.3171	0.3046	0.1215	0.3856	0.0216	0.5513	0.9923

Table 9. Summary of p-values for flexion-extension, internal-external, and abduction-adduction rotation angles during lateral SLS task for bilateral control (LR), ACLd, and PFP populations.

ACLd Group Medial

Data from the medially twisted SLS shows an increase in external rotation for 100% of the cycle and an increase in flexion for 100% of the cycle for ACLd participants compared to controls. There were no significant differences in abduction-adduction rotation angles. Three ACLd participant data sets were excluded for reasons mentioned in Section 4.1.

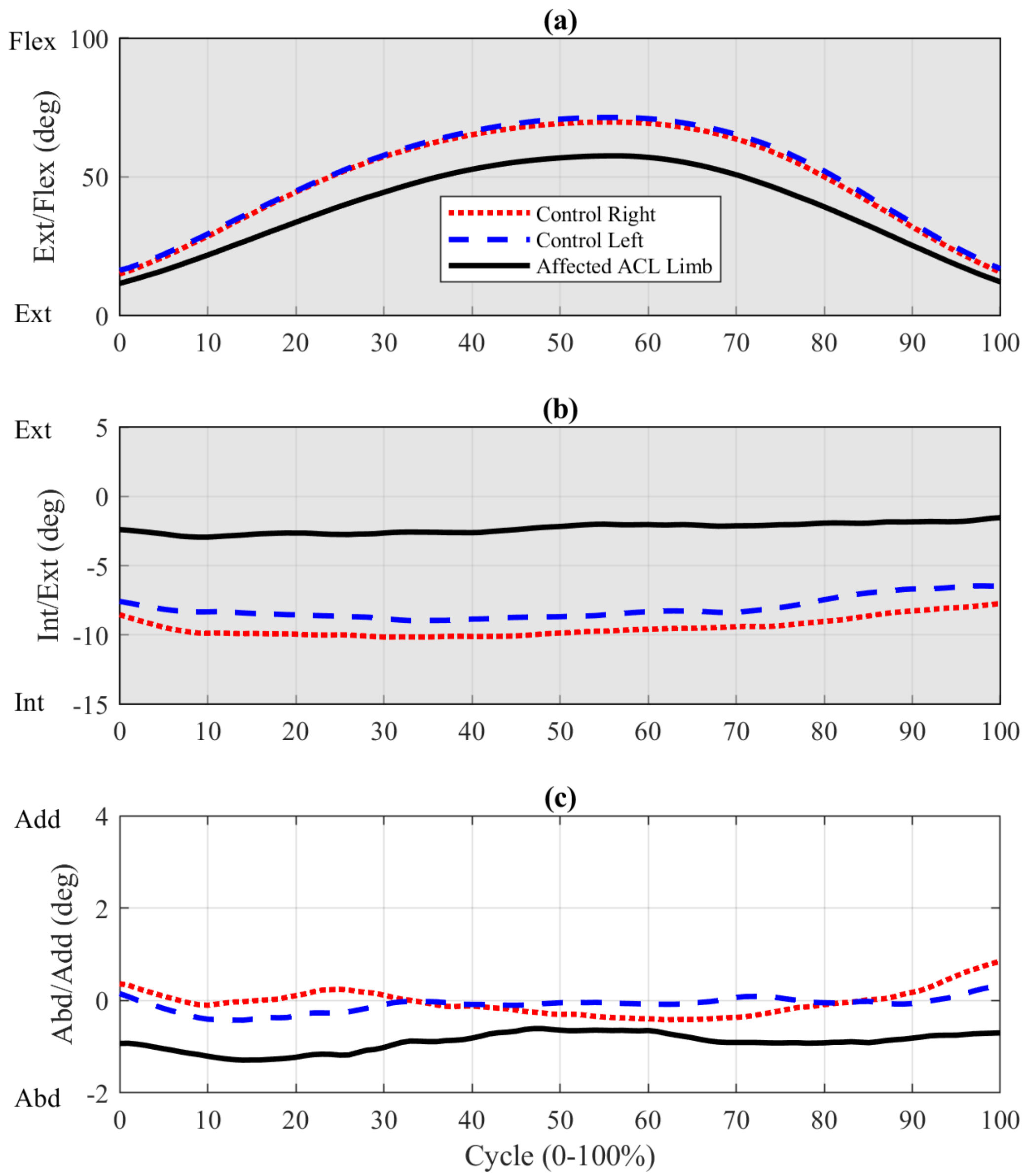

Figure 13. Rotation angles during medial SLS for ACLd group. (a) Flexion-extension. Significantly lower ACLd flexion rotation for 100% of the cycle. (b) Internal-external. Significantly less ACLd internal rotation for 100% of the cycle. (c) Abduction-adduction. Shaded regions indicate areas of significant differences.

ACL Group Lateral

Data from the laterally twisted SLS shows an increase in external rotation from 17-85% of the cycle and an increase in flexion from 9-94% of the cycle for ACLd participants compared to controls. There were no significant differences in abduction-adduction rotation angles. Three ACLd participant data sets were excluded for reasons mentioned in Section 4.1.

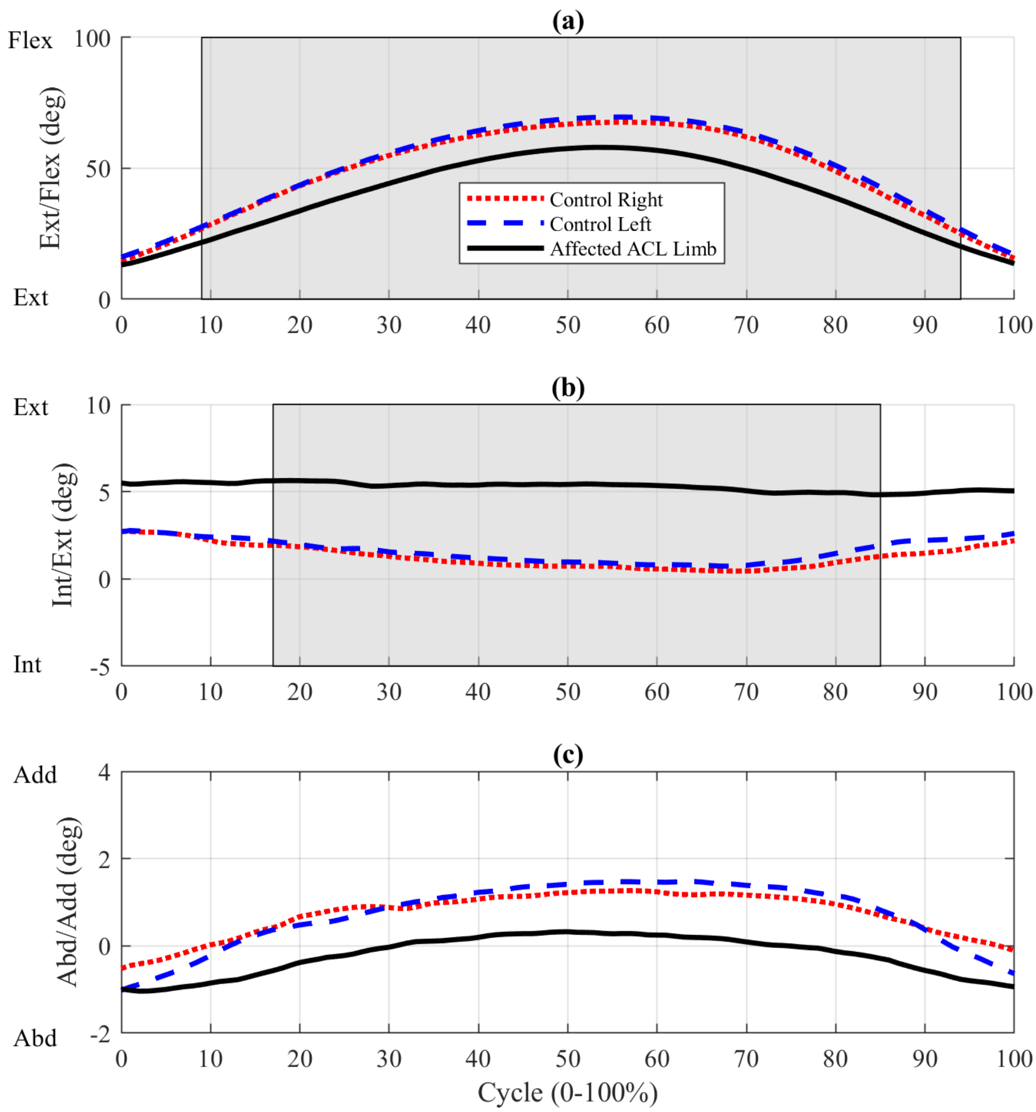

Figure 14. Rotation angles during lateral SLS for ACLd group. (a) Flexion-extension. Significantly lower ACLd flexion rotation between 9-94% of the cycle. (b) Internal-external. Significantly more ACLd external rotation between 17-85% of the cycle. (c) Abduction-adduction. Shaded regions indicate areas of significant differences.

PFP Group Medial

Data from the medially twisted SLS shows an increase in external rotation from 2-18%, 24-46%, and 68-75% and a decrease in flexion for 100% of the cycle for PFP participants compared to controls. There were no significant differences in abduction-adduction rotation angles. Two PFP participant data sets were excluded for reasons mentioned in Section 4.1.

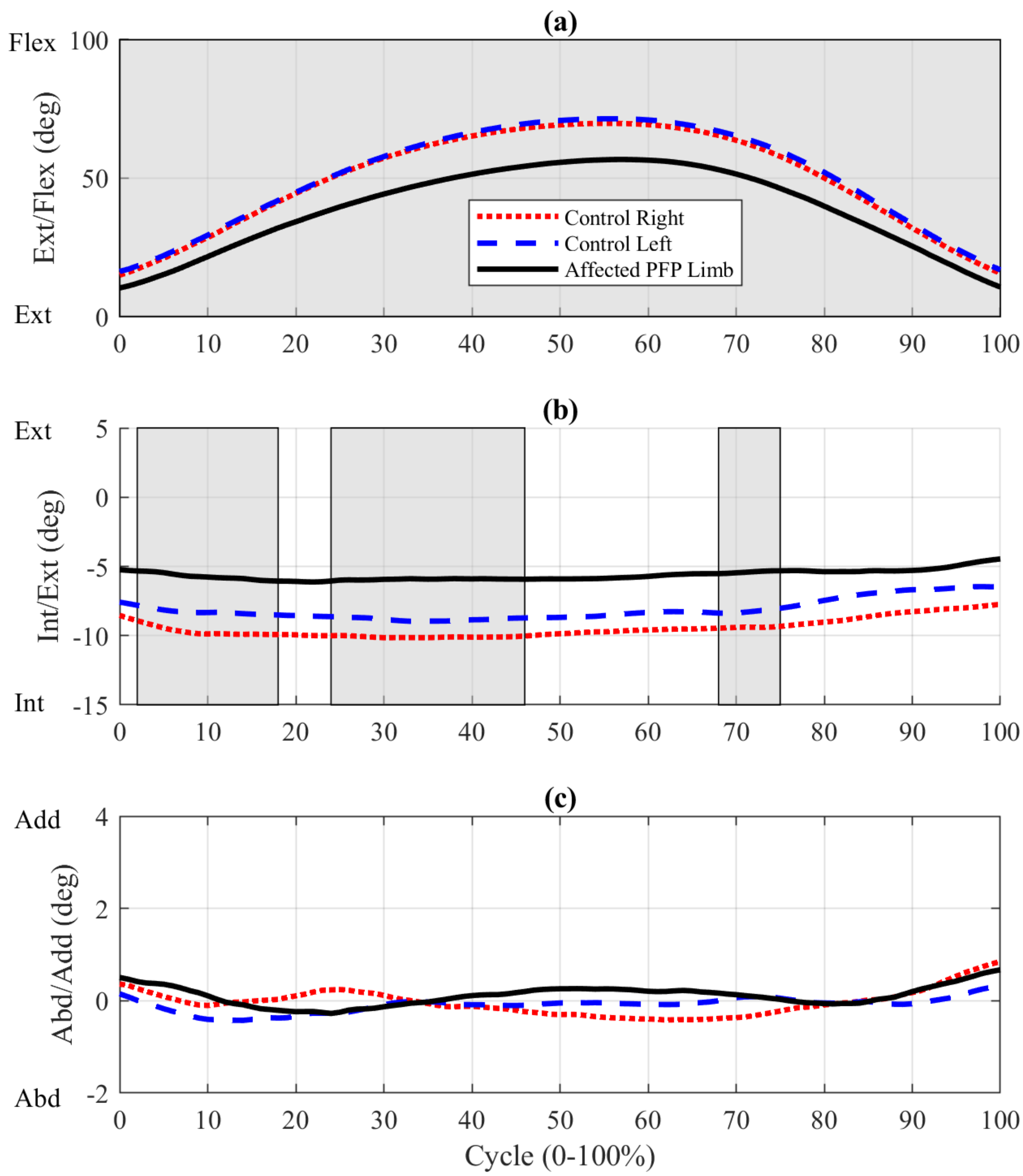

Figure 15. Rotation angles during medial SLS for PFP group. (a) Flexion-extension. Significantly lower PFP flexion rotation for 100% of the cycle. (b) Internal-external. Significantly less PFP internal rotation between 2-18%, 24-46%, and 68-75% of the cycle. (c) Abduction-adduction. Shaded regions indicate areas of significant differences.

PFP Group Lateral

Data from the laterally twisted SLS shows a decrease in flexion for 100% of the cycle for PFP participants compared to controls. There were no significant differences in abduction-adduction or internal-external rotation angles. One PFP participant data set was excluded for reasons mentioned in Section 4.1.

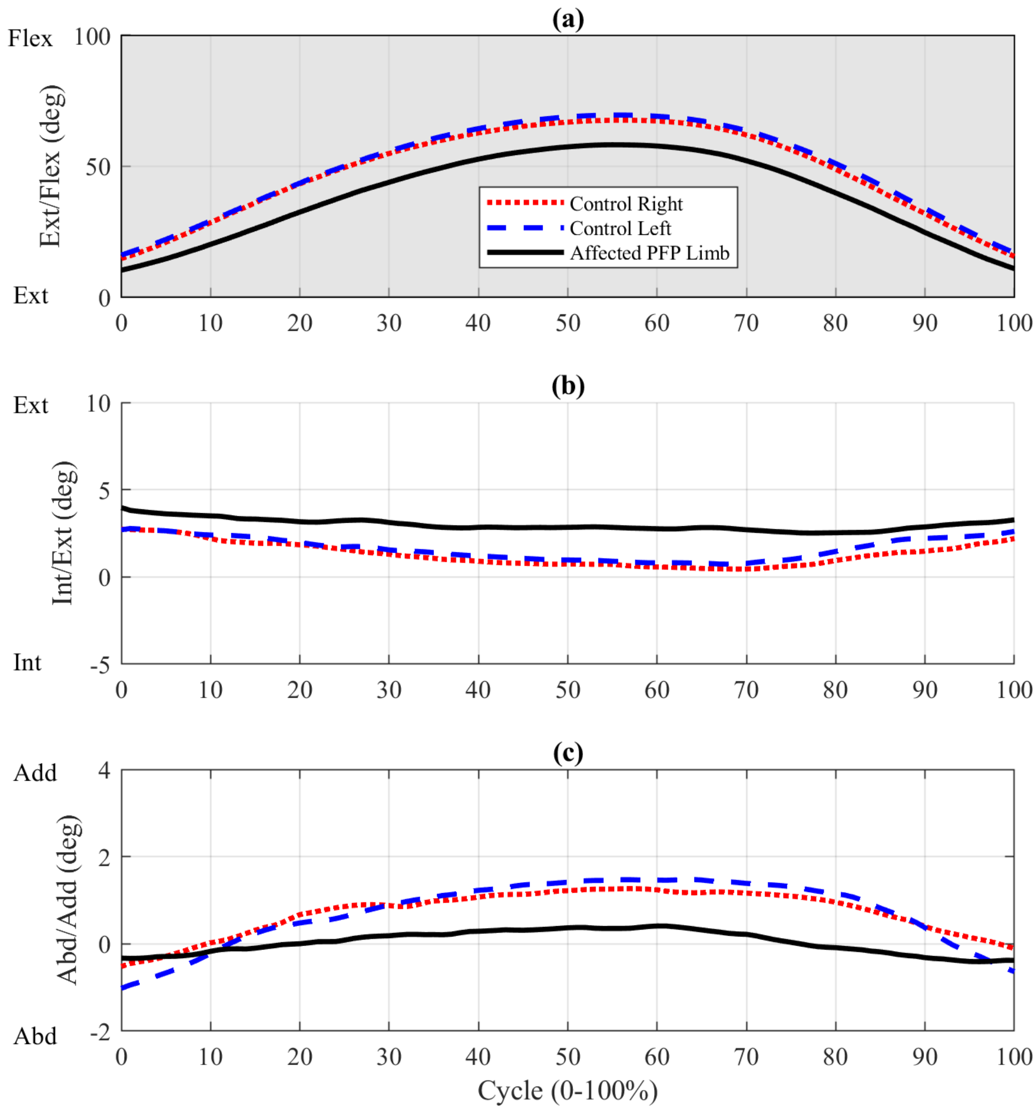

Figure 16. Rotation angles during lateral SLS for PFP group. (a) Flexion-extension. Significantly lower PFP flexion rotation for 100% of the cycle. (b) Internal-external. (c) Abduction-adduction. Shaded regions indicate areas of significant differences.

4.2 SimVitro testing

The results from the SimVitro testing were not true reflections of the MKATS device itself due to unperceived amounts of skin artifact and laxity in the cadaver knees compared to living participants. Further testing was done with simultaneous data collection during CT scans on live participants to compare joint angles calculated from geometries derived from the CT scan with joint angles output from the MKATS.

5. Discussion

These analyses may be limited as right and left control data were lumped together thus neglecting bilateral asymmetries. However, bilateral differences observed between control participants during the step up and over task were of a lesser magnitude than between control and clinical populations. Healthy individuals may have bilateral differences in kinematics related to asymmetries in muscle strength and flexibility[28] as shown in Figure 17. Rotation angles from the 3 step-up-and-over tasks from a representative control participant with bilateral asymmetrical internal-external rotation angles (a) and rotation angles from a representative control participant with relative symmetry between limbs (b). It has also been shown that there are inherent differences in side-to-side morphology and kinematics for healthy individuals during the gait cycle[6,13,28]. It was hypothesized that participant familiarity with the tasks may be a cause of the altered side-to-side kinematics during the step-up and over task. For all control participants, data was collected first on the right followed by the left, which is a study limitation. The participants may have been more familiar with the tasks the second time and thus performed them faster or with less hesitation. In future studies, alternating which leg is tested first for each participant may reduce biases related to task familiarity.

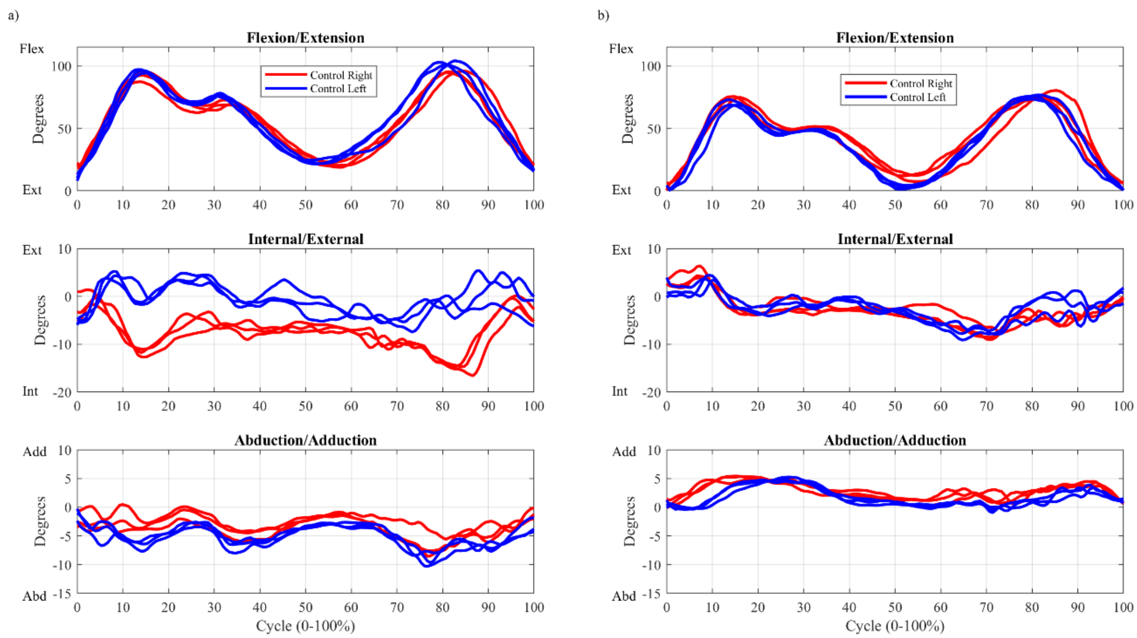

Figure 17. Rotation angles from the 3 step-up-and-over tasks from a representative control participant with bilateral asymmetrical internal-external rotation angles (a) and rotation angles from a representative control participant with relative symmetry between limbs (b).

While tasks such as the lateral step-down, step-up and over, and Y balance tests were all selected from standard tests, the large statistically significant differences between healthy control and clinical populations during SLS with rotation suggest that such a task may capture pathological kinematics well. However, more work needs to be done to establish a standardized testing method so that clinical significance can be applied to metrics obtained from such tasks. Some participants chose to place their contralateral toes on the ground for support while others did not. Additionally, placement of the contralateral leg varied. One way to make this test more standard would be give explicit instruction on where to place the contralateral leg and how much to rotate.

5.1 Relevance to ACL Population

Studies evaluating knee motion in ACLd or ACL reconstructed populations have varied and often report conflicting results[1,11,13,18,67]. Many studies have observed more internal rotation with increased flexion, but it should be noted that most of these are cadaver studies which are limited to testing passive stability[67].These studies can measure relative bone motion very accurately, but often neglect the influence of muscle forces. Some gait studies on healthy populations found the knee to be in internal rotation throughout the cycle[1,11] while others found the knee to be in external rotation throughout the cycle[28,31,42]. Other studies found more external rotation in the stance phase with more internal rotation in the swing phase[13,25,36]. These studies all used instrumented motion analysis, but the algorithms used for data processing varied. In this study, ACLd patients had increased external rotation for ≥ 90% of LSD, SUO, and Y-balance tasks. The ACLd population also had decreased peak flexion during flexed periods for dynamic tasks which may be another indicator of decreased stability of the joint and aligns with a systemic review by Zhang et al[68].

In all tasks, knee arthrokinematics result from external knee loading and muscle forces as well as geometric and soft tissue constraints[8,12]. Patients with a history of ACL deficiency have not only a change in passive support at the knee, but changes to motor control and muscle activation as well[19,22]. The observed changes in kinematics are likely a combination of many things including the loss in passive support from the ACL, the loss of mechanoreceptors near the TF joint, and subsequent altered input from the central nervous system[19,22]. Such altered kinematics are indicative of instability, changing compensation mechanisms, and altered loading of the joint[22]. One cadaver study found that sectioning of the ACL increased forces carried by both the lateral meniscus and the medial femoral condyle through cartilage-to-cartilage contact[45].

Increased antagonistic muscle activation can lead to increased compressive forces on the knee which can accelerate progression of cartilage degeneration[18]. Such abnormalities in kinematics and changes in the contact pattern of the articular surfaces can be aggravated with extensive cycles of loading and lead to post-traumatic osteoarthritis[18,47]. These long-term degenerative changes typically require additional costly treatment regardless of if the patient was treated surgically or conservatively[44].

One limitation of this data set includes the range of injury timing. Most participants were injured within one year. However, there were six participants whose initial injury occurred more than a year prior to data collection and two whose initial injury occurred more than a decade prior. Injury timing may affect the compensation mechanisms that individuals develop following injury[18]. While most initial swelling post injury should be gone within a week, studies have found increased levels of inflammatory cytokines and biomarkers associated with increased collagen turnover up to a decade after injury[26]. One patient was injured one week prior to data collection and may have had increased swelling or pain that further altered their performance[26]. A patient who ruptured their ACL 3 weeks prior may have different compensation patterns than one who has been ACLd for a year with rehabilitation/physical therapy before surgical interventions[18].

Triplanar metrics such as those used in this study may be useful for tracking progress of both conservative and surgical treatments of ACL related pathologies. Metrics that align more closely with normative data can indicate that an athlete is ready to return to sport[4]. Additionally, such kinematic metrics may be useful for screening uninjured athletes for ACL injury risk[43]. It has been found that smaller ACLs are associated with less linear stiffness[10], lower load at failure[10], and greater anterior knee laxity[65]. As those with greater knee laxity have been associated with a greater ACL injury risk[58], objective and noninvasive metrics could be used in preventative training protocols.

5.2 Relevance to PFP Population

Patellofemoral pain syndrome is typically a diagnosis of exclusion after other pathologies have been ruled out[46]. One of the most accepted symptoms is retropatellar or peripatellar pain that has gone on for more than 3 months[5,15,41]. While the primary characteristics are altered patellar tracking and increased lateral stress at the patellofemoral joint, the cause of these characteristics is multifactorial[5]. As such, there is a wide range of symptoms and severity within those diagnosed with PFP. Most patients have soft tissue swelling which can progress into severe arthritic changes[41,66]. One suggested mechanism is that increased stress at the patellofemoral joint during loaded flexed activity transmits through the cartilage to nociceptors in the subchondral bone thus causing pain[41]. Typical criterion for diagnosis includes pain during loaded functional tasks such as those previously mentioned in Section 1[41,66]. While a correlation between kinematics and pain has been associated, there is a debate over whether poor kinematics lead to pain or whether pain led to compensation mechanisms to decrease the patellofemoral joint load[5].

Due to the complex definition of the pathology and range of severity, there is a paucity of studies looking at dynamics in PFP populations. Barton et al. found altered dynamics including a reduction in gait velocity, reduced internal hip rotation, and increased pronation of the foot[5]. While peak flexion is not consistently different in level walking, other studies have found reduced peak flexion on stair ascent and there is general agreement that altered kinematics are related to increased patellofemoral joint loads[17,66]. This history supports the findings observed with the MKATS as all tasks produced some degree of decreased peak flexion and decreased internal rotation.

Another factor to consider in the kinematics of those with PFP, is muscle activation. Resisted isometric quadriceps femoris muscle activation is another common test utilized in diagnosis and treatment of PFP[55,66]. Lankhorst et al found that quadriceps strength in PFP populations was considerably diminished using dynamometry[40]. It has been suggested that decreased quadriceps activation may be related to inhibited central neural drive as a result of pain feedback[59]. Studies utilizing electromyography have found that some PFP populations have delayed vastus medialis obliquus activation relative to the vastus lateralis[17]. Such activation patterns may alter the alignment of the patella thus contributing to increased pain and development of osteoarthritis[16,66]. Further investigation is needed to understand the relationship between the symptom of pain and the factors of joint loading, muscle activation, and kinematics.

While treatment options for PFP are usually nonsurgical, objective triplanar metrics can be useful to physical therapists treating PFP to track patient progression. Proper treatment of PFP may be able to correct loading patterns and prevent further degenerative changes[66].

5.3 Further Device Development

Discussions with physical therapists, athletic trainers, and other orthopedic clinicians during interviews for the NSF Innovation Corps bootcamp confirmed that potential users desire objective assessment of knee function and that tibial rotation is difficult to assess visually. Some of the current limitations they experience are adequate objective measures to show patient improvement in documentation for payers, costs of instrumented assessment tools, standardized metrics, and proper space to perform assessments. Part of a physical therapist’s job is to objectively assess patient progression and advocate for their patients to healthcare payers and other parties. A device such as the MKATS can provide objective documentable metrics, biofeedback for the patient, dynamic realistic assessments for sports, and justification for marketing their services. These metrics can help clinicians decide if the patient is ready for discharge, if the patient is ready to return to sports or other activities, and if the intervention is effective or not. Within the customer segments interviewed the following should be considered with further MKATS development:

- The device is portable and space efficient.
- The device is inexpensive (~$2,000).
- Data from the device is validated and standardized.
- The device provides dynamic real time data with a straightforward user interface.
- Objective data from the device can easily be documented for insurance.

In addition to improving the current device which has three adult sizes, the femur and tibia fixtures can be altered to fit more populations such as pediatric populations. An example of a smaller clamp with less side material is shown in Figure 18.

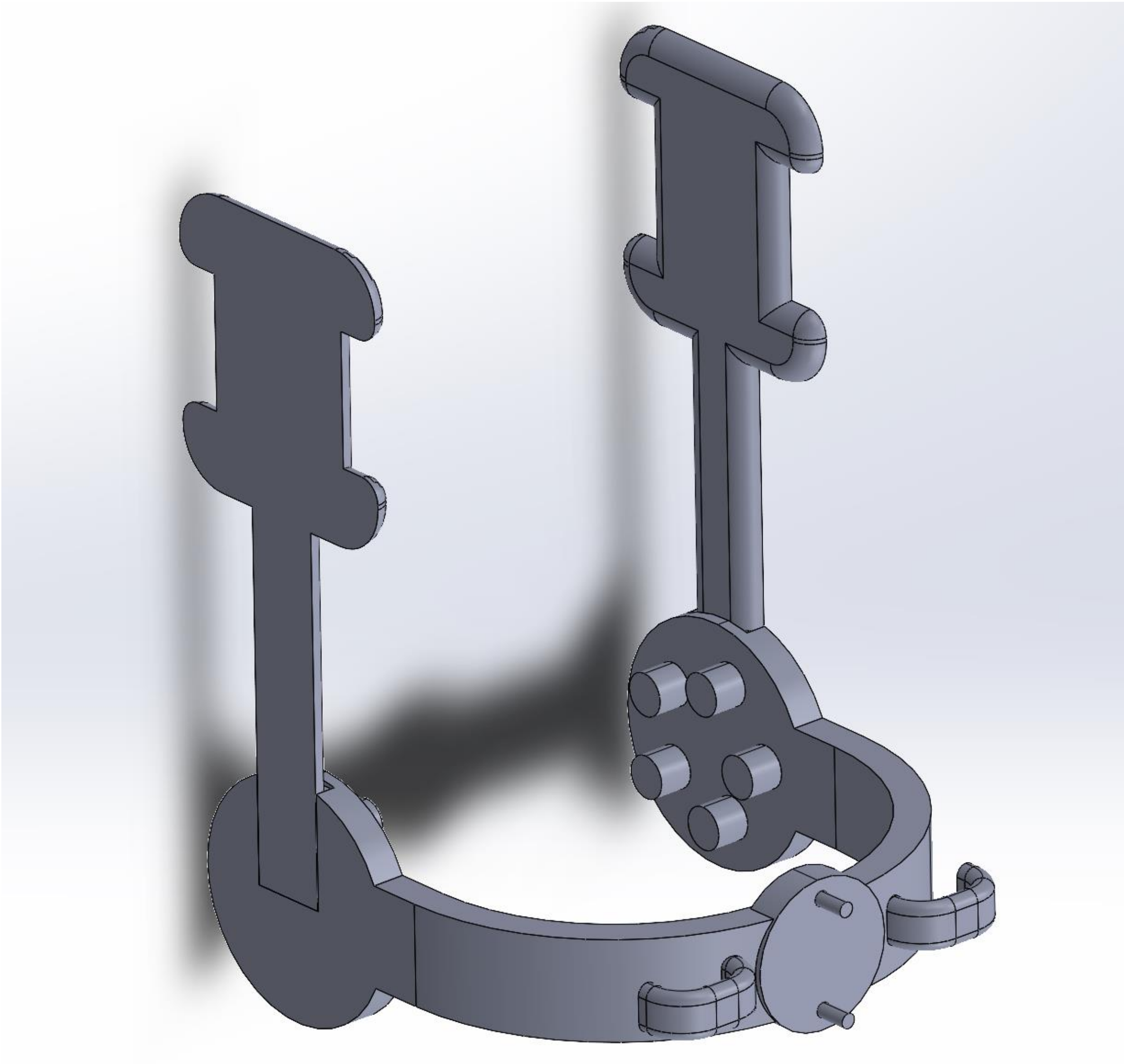

Figure 18. Computer-aided design for one pediatric clamp size in SolidWorks. Note that the design was altered to be overall smaller and the sides were trimmed down to reduce bulk and be more accommodating to scissoring action.

6. Conclusion

The MKATS device was able to measure triplanar joint angles for more than 60 healthy and clinical participants. Such data is greatly beneficial for clinicians seeking to evaluate pathologies of the knee such as ACL deficiencies and PFP. This could be extremely useful as an objective metric for determining when fit to return to sport and justifying continuing treatment in physical therapy. Easily accessible objective metrics allow clinicians to justify compensation from healthcare payers (e.g. insurance companies) and track treatment progression.

7. References

1. Akbarshahi M, Schache AG, Fernandez JW, et al. Non-invasive assessment of soft-tissue artifact and its effect on knee joint kinematics during functional activity. *Journal of Biomechanics.* 2010;43(7):1292-1301.
2. Amiri S, Wilson DR. A computational modeling approach for investigating soft tissue balancing in bicruciate retaining knee arthroplasty. *Computational and mathematical methods in medicine.* 2012;2012:652865-652865.
3. Arilla FV, Yeung M, Bell K, et al. Experimental Execution of the Simulated Pivot-Shift Test: A Systematic Review of Techniques. *Arthroscopy.* 2015;31(12):2445-2454.e2442.
4. Ashigbi EYK, Banzer W, Niederer D. Return to Sport Tests' Prognostic Value for Reinjury Risk after Anterior Cruciate Ligament Reconstruction: A Systematic Review. *Medicine and Science in Sports and Exercise.* 2020;52(6):1263-1271.
5. Barton CJ, Levinger P, Webster KE, Menz HB. Walking kinematics in individuals with patellofemoral pain syndrome: A case–control study. *Gait & Posture.* 2011;33(2):286-291.
6. Benoit D, Ramsey D, Lamontagne M, et al. In vivo knee kinematics during gait reveals new rotation profiles and smaller translations. *Clinical Orthopaedics and Related Research.* 2007(454):81-88.
7. Benoit DL, Ramsey DK, Lamontagne M, et al. Effect of skin movement artifact on knee kinematics during gait and cutting motions measured in vivo. *Gait Posture.* 2006;24(2):152-164.
8. Bernard M, Pappas E, Georgoulis A, et al. Risk of overconstraining femorotibial rotation after anatomical ACL reconstruction using bone patella tendon bone autograft. *Archives of Orthopaedic and Trauma Surgery.* 2020;140(12):2013-2020.
9. Buckwalter JA. Sports, joint injury, and posttraumatic osteoarthritis. *J Orthop Sports Phys Ther.* 2003;33(10):578-588.
10. Chandrashekar N, Slauterbeck J, Hashemi J. Sex-based differences in the anthropometric characteristics of the anterior cruciate ligament and its relation to intercondylar notch geometry: a cadaveric study. *Am J Sports Med.* 2005;33(10):1492-1498.
11. Chao EY, Laughman RK, Schneider E, Stauffer RN. Normative data of knee joint motion and ground reaction forces in adult level walking. *Journal of Biomechanics.* 1983;16(3):219-233.
12. Chaudhari A, Briant P, Bevill S, Koo S, Andriacchi T. Knee kinematics, cartilage morphology, and osteoarthritis after ACL injury. *Medicine and Science in Sports and Exercise.* 2008;40(2):215-222.
13. Clement J, Toliopoulos P, Hagemeister N, et al. Healthy 3D knee kinematics during gait: Differences between women and men, and correlation with x-ray alignment. *Gait & Posture.* 2018;64:198-204.
14. Cole MH, Grimshaw PN. The Biomechanics of the Modern Golf Swing: Implications for Lower Back Injuries. *Sports Med.* 2016;46(3):339-351.
15. Cook C, Hegedus E, Hawkins R, Scovell F, Wyland D. Diagnostic accuracy and association to disability of clinical test findings associated with patellofemoral pain syndrome. *Physiother Can.* 2010;62(1):17-24.
16. Crossley KM. Recent advances in understanding the biomechanics of patellofemoral pain. *Journal of Foot and Ankle Research.* 2011;4(1):I3.

17. Crossley KM, Cowan SM, Bennell KL, McConnell J. Knee flexion during stair ambulation is altered in individuals with patellofemoral pain. *Journal of Orthopaedic Research.* 2004;22(2):267-274.
18. Gao B, Cordova M, Zheng N. Three-dimensional joint kinematics of ACL-deficient and ACL-reconstructed knees during stair ascent and descent. *Human Movement Science.* 2012;31(1):222-235.
19. Gokeler A, Neuhaus D, Benjaminse A, Grooms DR, Baumeister J. Principles of Motor Learning to Support Neuroplasticity After ACL Injury: Implications for Optimizing Performance and Reducing Risk of Second ACL Injury. *Sports Med.* 2019;49(6):853-865.
20. Gokeler A, Welling W, Zaffagnini S, Seil R, Padua D. Development of a test battery to enhance safe return to sports after anterior cruciate ligament reconstruction. *Knee Surg Sports Traumatol Arthrosc.* 2017;25(1):192-199.
21. Grood ES, Suntay WJ. A joint coordinate system for the clinical description of three-dimensional motions: application to the knee. *J Biomech Eng.* 1983;105(2):136-144.
22. Grooms DR, Page SJ, Nichols-Larsen DS, et al. Neuroplasticity Associated With Anterior Cruciate Ligament Reconstruction. *Journal of Orthopaedic & Sports Physical Therapy.* 2017;47(3):180-189.
23. Record #78 is using an undefined reference type. If you are sure you are using the correct reference type, the template for that type will need to be set up in this output style.
24. Hall J, Guess T. The effect of an ankle–foot orthosis on tibiofemoral motion during step-up and step-down in healthy adults. *Prosthetics and Orthotics International.* 2021.
25. Han SY, Cheng G, Xu P. Three-dimensional lower extremity kinematics of Chinese during activities of daily living. *Journal of Back and Musculoskeletal Rehabilitation.* 2015;28(2):327-334.
26. Harkey MS, Luc BA, Golightly YM, et al. Osteoarthritis-related biomarkers following anterior cruciate ligament injury and reconstruction: a systematic review. *Osteoarthritis Cartilage.* 2015;23(1):1-12.
27. Hull ML. Coordinate system requirements to determine motions of the tibiofemoral joint free from kinematic crosstalk errors. *Journal of Biomechanics.* 2020;109:109928.
28. Ino T, Ohkoshi Y, Maeda T, et al. Side-to-side differences of three-dimensional knee kinematics during walking by normal subjects. *Journal of Physical Therapy Science.* 2015;27(6):1803-1807.
29. Ithurburn MP, Altenburger AR, Thomas S, et al. Young athletes after ACL reconstruction with quadriceps strength asymmetry at the time of return-to-sport demonstrate decreased knee function 1 year later. *Knee Surgery Sports Traumatology Arthroscopy.* 2018;26(2):426-433.
30. James SL, Abate D, Abate KH, et al. Global, regional, and national incidence, prevalence, and years lived with disability for 354 diseases and injuries for 195 countries and territories, 1990–2017: a systematic analysis for the Global Burden of Disease Study 2017. *The Lancet.* 2018;392(10159):1789-1858.
31. Kadaba MP, Ramakrishnan HK, Wootten ME, et al. Repeatability of kinematic, kinetic, and electromyographic data in normal adult gait. *Journal of Orthopaedic Research.* 1989;7(6):849-860.
32. Kaeding CC, Léger-St-Jean B, Magnussen RA. Epidemiology and Diagnosis of Anterior Cruciate Ligament Injuries. *Clin Sports Med.* 2017;36(1):1-8.

33. Keizer MNJ, Otten E. Technical note: sensitivity analysis of the SCoRE and SARA methods for determining rotational axes during tibiofemoral movements using optical motion capture. *Journal of Experimental Orthopaedics.* 2020;7(1).
34. Khan N, Dockter E, Fithian D, al e. Development of Arthrometry. In: *Rotary Knee Instability: An Evidence Based Approach.* Springer International Publishing; 2016:115-129.
35. Khan R, Lie D, Cashman P, Thomas R, Amis A. Measurement of laxity in the anterior cruciate ligament-deficient knee: a comparison of three different methods in vitro. *Proceedings of the Institution of Mechanical Engineers Part H-Journal of Engineering in Medicine.* 2007;221(H6):653-663.
36. Kim HY, Kim KJ, Yang DS, et al. Screw-Home Movement of the Tibiofemoral Joint during Normal Gait: Three-Dimensional Analysis. *Clin Orthop Surg.* 2015;7(3):303-309.
37. Koontz AM, McCrory JL, Cham R, Yang Y, Wilkinson M. Rehabilitation Biomechanics. *Wiley Encyclopedia of Biomedical Engineering.* 2006.
38. Kotsifaki A, Korakakis V, Whiteley R, Van Rossom S, Jonkers I. Measuring only hop distance during single leg hop testing is insufficient to detect deficits in knee function after ACL reconstruction: a systematic review and meta-analysis. *British Journal of Sports Medicine.* 2020;54(3):139.
39. Kozanek M, Hosseini A, Van de Velde SK, et al. Kinematic evaluation of the step-up exercise in anterior cruciate ligament deficiency. *Clinical Biomechanics.* 2011;26(9):950-954.
40. Lankhorst NE, van Middelkoop M, Crossley KM, et al. Factors that predict a poor outcome 5–8 years after the diagnosis of patellofemoral pain: a multicentre observational analysis. *British Journal of Sports Medicine.* 2016;50(14):881.
41. Leibbrandt DC, Louw Q. The development of an evidence-based clinical checklist for the diagnosis of anterior knee pain. *S Afr J Physiother.* 2017;73(1):353.
42. Li J, Wyss UP, Costigan PA, Deluzio KJ. An integrated procedure to assess knee-joint kinematics and kinetics during gait using an optoelectric system and standardized x-rays. *Journal of Biomedical Engineering.* 1993;15(5):392-400.
43. Lin CF, Gross M, Ji C, et al. A stochastic biomechanical model for risk and risk factors of non-contact anterior cruciate ligament injuries. *J Biomech.* 2009;42(4):418-423.
44. Mather RC, Koenig L, Kocher MS, et al. Societal and Economic Impact of Anterior Cruciate Ligament Tears. *Journal of Bone and Joint Surgery-American Volume.* 2013;95A(19):1751-1759.
45. McDonald LS, Boorman-Padgett J, Kent R, et al. ACL Deficiency Increases Forces on the Medial Femoral Condyle and the Lateral Meniscus with Applied Rotatory Loads. *Journal of Bone and Joint Surgery-American Volume.* 2016;98(20):9.
46. McKenzie K, Galea V, Wessel J, Pierrynowski M. Lower Extremity Kinematics of Females With Patellofemoral Pain Syndrome While Stair Stepping. *Journal of Orthopaedic & Sports Physical Therapy.* 2010;40(10):625-632.
47. Mootanah R, Imhauser CW, Reisse F, et al. Development and validation of a computational model of the knee joint for the evaluation of surgical treatments for osteoarthritis. *Computer Methods in Biomechanics and Biomedical Engineering.* 2014;17(13):1502-1517.
48. Moraes GF, Antunes AP. Musculoskeletal disorders in professional violinists and violists. Systematic review. *Acta Ortop Bras.* 2012;20(1):43-47.

49. Moulton SG, Turnbull TL, Kennedy NI, LaPrade RF, Prodromos CC. 112 - Functional Bracing for Anterior Cruciate Ligament Injuries: Current State and Future Direction. In: *The Anterior Cruciate Ligament (Second Edition).* Elsevier; 2018:459-461.e451.
50. Musahl V, Karlsson J. Anterior Cruciate Ligament Tear. *New England Journal of Medicine.* 2019;380(24):2341-2348.
51. Nesbit SM, Serrano M. Work and power analysis of the golf swing. *J Sports Sci Med.* 2005;4(4):520-533.
52. Papadopoulos K, Stasinopoulos D, Ganchev D. A systematic review of reviews in patellofemoral pain syndrome. Exploring the risk factors, diagnostic tests, outcome measurements and exercise treatment. *Open Sports Medicine Journal.* 2015;9:7-17.
53. Piva SR, Fitzgerald K, Irrgang JJ, et al. Reliability of measures of impairments associated with patellofemoral pain syndrome. *BMC Musculoskeletal Disorders.* 2006;7(1):33.
54. Rambaud AJM, Rossi J, Neri T, Samozino P, Edouard P. Evolution of Functional Recovery using Hop Test Assessment after ACL Reconstruction. *International Journal of Sports Medicine.* 2020;41(10):696-704.
55. Roush MB, Sevier TL, Wilson JK, et al. Anterior Knee Pain: A Clinical Comparison of Rehabilitation Methods. *Clinical Journal of Sport Medicine.* 2000;10(1).
56. Saravia A, Cabrera S, Molina CR, Pacheco L, Muñoz G. Validity of the Genourob arthrometer in the evaluation of total thickness tears of anterior cruciate ligament. *J Orthop.* 2020;22:203-206.
57. Smith BE, Selfe J, Thacker D, et al. Incidence and prevalence of patellofemoral pain: A systematic review and meta-analysis. *PLOS ONE.* 2018;13(1):e0190892.
58. Sturnick DR, Vacek PM, DeSarno MJ, et al. Combined Anatomic Factors Predicting Risk of Anterior Cruciate Ligament Injury for Males and Females. *American Journal of Sports Medicine.* 2015;43(4):839-847.
59. Thomeé R, Renström P, Karlsson J, Grimby G. Patellofemoral pain syndrome in young women. *Scandinavian Journal of Medicine & Science in Sports.* 1995;5(4):245-251.
60. Timaran LI, Timaran CH, Scott CK, et al. Dual fluoroscopy with live-image digital zooming significantly reduces patient and operating staff radiation during fenestrated-branched endovascular aortic aneurysm repair. *J Vasc Surg.* 2021;73(2):601-607.
61. Uzuner S, Rodriguez ML, Li L, Kucuk S. Dual fluoroscopic evaluation of human tibiofemoral joint kinematics during a prolonged standing: A pilot study. *Engineering Science and Technology, an International Journal.* 2019;22(3):794-800.
62. Van de Velde SK, Bingham JT, Hosseini A, et al. Increased Tibiofemoral Cartilage Contact Deformation in Patients With Anterior Cruciate Ligament Deficiency. *Arthritis and Rheumatism.* 2009;60(12):3693-3702.
63. Vaudreuil NJ, Rothrauff BB, de Sa D, Musahl V. The Pivot Shift: Current Experimental Methodology and Clinical Utility for Anterior Cruciate Ligament Rupture and Associated Injury. *Curr Rev Musculoskelet Med.* 2019;12(1):41-49.
64. Visentin P, Li S, Tardif G, Shan G. Unraveling mysteries of personal performance style; biomechanics of left-hand position changes (shifting) in violin performance. *PeerJ.* 2015;3:e1299.
65. Wang H-M, Shultz SJ, Ross SE, et al. Relationship of Anterior Cruciate Ligament Volume and T2* Relaxation Time to Anterior Knee Laxity. *Orthopaedic journal of sports medicine.* 2021;9(2):2325967120979986-2325967120979986.

66. Willy RW, Hoglund LT, Barton CJ, et al. Patellofemoral Pain. *Journal of Orthopaedic & Sports Physical Therapy.* 2019;49(9).
67. Wünschel M, Müller O, Lo J, Obloh C, Wülker N. The anterior cruciate ligament provides resistance to externally applied anterior tibial force but not to internal rotational torque during simulated weight-bearing flexion. *Arthroscopy.* 2010;26(11):1520-1527.
68. Zhang L, Liu G, Han B, et al. Knee Joint Biomechanics in Physiological Conditions and How Pathologies Can Affect It: A Systematic Review. *Applied Bionics and Biomechanics.* 2020;2020:22.